



UNIVERSITAT DE BARCELONA

Final Degree Project
Biomedical Engineering Degree

**Ventricular Extrasystole Ablation:
electrophysiological characterization
according to its origin**

Barcelona, June 14th, 2021
Author: Eduard Solé Galindo
Tutor: Paz Garre Anguera de Sojo

INDEX

1. INTRODUCTION	5
1.1. OBJECTIVES	6
1.2. JUSTIFICATION OF THE PROJECT	7
2. BACKGROUND	7
2.1. PREMATURE VENTRICULAR COMPLEXES (PVCs)	7
2.1.1. HISTORICAL STUDIES	7
2.1.2. CLINICAL IMPLICATIONS	8
2.1.3. TREATMENT OF PVCs	8
2.1.4. APPLICATIONS OF RF ABLATION TO PVCs.	11
2.2. INTRACAVITARY ELECTRICAL SIGNALS	13
2.2.1. UNIPOLAR AND BIPOLAR SIGNALS	13
2.3. PVC MAPPING	16
2.3.1. NAVIGATION SYSTEMS	16
2.3.1. ACTIVATION MAPPING	19
2.3.3. STATE OF THE SITUATION	22
3. MARKET ANALYSIS	23
4. CONCEPTION ENGINEERING	24
4.1. TALKING POINTS	24
4.2. POSSIBLE SOLUTIONS	24
4.3. PROPOSED SOLUTION:	26
5. DETAILED ENGINEERING	26
5.1. MATERIALS	26
5.2. METHODS	27
5.2.1. OVERVIEW	27
5.2.2. SEGMENTATION OF THE MAPS	28
5.2.3. MAP PROCESSING	29
5.2.4. STUDY OF THE POINTS	30
5.2.5. USE OF SPSS	31
5.3. RESULTS	32
5.3.1. BIPOLAR SIGNALS.	32
5.3.2. UNIPOLAR SIGNAL	34
5.3.3. OTHER OBSERVATIONS	36
5.4. DISCUSSION	37
5.5. LIMITATIONS OF OUR STUDY	39
6. EXECUTION CHRONOGRAM	39

6.1.	WORK BREAKDOWN STRUCTURE (WBS)	39
6.1.2.	CODING THE TASKS	41
6.1.3.	DEFINITION OF THE TIMES:	42
6.2.	DEPENDENCY MATRIX	43
6.3.	PERT DIAGRAM	43
6.4.	GANTT DIAGRAM	45
7.	TECHNICAL VIABILITY	47
8.	ECONOMIC VIABILITY	48
9.	LAWS TO WHICH THE STUDY IS SUBJECTED	48
10.	CONCLUSIONS AND FUTURE LINES	48
11.	BIBLIOGRAPHY	49
12.	ANNEXES	55
1.	CARDIAC CONDUCTION SYSTEM	55
2.	ARRHYTHMIAS	56
3.	DIAGNOSIS OF ARRHYTHMIAS	56
4.	PHARMACOLOGICAL TREATMENT OF ARRHYTHMIAS	58
5.	RPY NOTATION	59

Abstract

Introduction. Premature Ventricular Complexes (PVCs) are a frequent non-severe cardiac condition that in some cases can be malignant, as they may result in structural cardiomyopathies or even sudden death, and need treatment. For pharmacoresistant PVCs, catheter ablation is used with a success rate between 50-90% for PVC burden reduction.

The catheter used has a set of electrodes used to measure intracavitary signals.

Hypothesis and objectives. Electrophysiological characteristics of the PVCs could be used to characterize the signals expected at different ventricular structures and assess the outcome of the ablation in real-time.

Material and methods. Using CARTO3 (Remote Magnetic Navigation) we studied 29 PVCs (24 patients), from the Arrhythmia Unit of the Hospital Clinic of Barcelona. We characterized unipolar and bipolar electrograms by measuring amplitudes, precocities and unipolar negative deflections, and the most precocious isochrone at different cardiac points: Left ventricle (LV), Right ventricle (RV), Pulmonary artery (AP), Summit(S) and cusps (C).

Results. Bipolar signals: the most precocious locations were RV and S, differences between RV-S (24.2 ms vs 43.3 p=0.0017) and C-S (26.6 vs 43.3 p=0.0104). LV showed the largest bipolar amplitude (5.65 mV), S the lowest (0.26).

Areas showing largest number of unipolar negative deflections were RV (n=1.43), C (n=1.53) and AP (n=1.65), being significantly different from S (n=0.95, p=0.0445, 0.0092, 0.00119, respectively).

The steepest slope at LV (0.3 mV/ms), flattest at S (0.0297), finding significant differences LV-RV (p=0.0493).

Unipolar precocities were significantly different between RV (26.9 ms) and LV (16.2, p=0.0002).

Conclusion. Relations can be found between intracavitary ablation signals and ventricular structures. Differences in precocities between ventricles could be used as a marker to assess the state of intervention.

More studies are needed to characterize ventricular substructures and to assess the long-term outcome of the procedure.

1. INTRODUCTION

What is there in common between The Beach Boys, your heart and Lynyrd Skynyrd?

As confusing as this question may seem at first glance, from 4^[1] weeks after our conception until the day we die, human hearts beat at a given pace. This pace is set by the cardiac conduction system (Annex 1) and ranges between **60 beats per minute** (which is the same rhythm as the song Caroline No from The Beach Boys) and **100^[2] beats per minute** (which is the same amount as in the song Sweet Home Alabama by Lynyrd Skynyrd). A rhythmic heartbeat in this range is considered normal and this is known as the **sinus rhythm**.

But what happens when our ventricles do not follow the rhythm? This is the case for a particular kind of arrhythmia known as **Ventricular Extrasystole or Premature ventricular Complex (PVC)^[3]**. PVCs are based on the apparition of ventricular **foci**, that acquire automatism and can generate depolarizations that will result in a **contraction of the ventricle between sinus beats**. Adding a ventricular beat between the ones set by the normal SA rhythm.

It has been estimated that **at least one person out of every 2** will suffer, at some point in their lives, from occasional PVC episodes^{[4][5][6]}.

Ventricular Extrasystoles can be detected in patients without apparent structural heart diseases. Some people might even be asymptomatic to this condition or only present isolated episodes with no continuity.

PVCs are not usually considered as a malignant condition and it results in a reversible type of cardiomyopathy. Yet, **some PVCs can turn out to be malignant**, in that case, this additional beat(s) can trigger the development of **structural cardiomyopathies** or even be the cause of **sudden death**.

Such a large number of people experimenting this condition could not have been let go by medical research and it has been studied since 1959^[7].

Nowadays, the most effective intervention for PVC treatment is the **catheter ablation**. This technique consists in the creation of a lesion in the cardiac tissue of the patient. The resulting scar becomes an area of non-conductive tissue, in an attempt to stop the transmission of the electrical stimuli that cause the PVCs.

Catheter ablation has a **success rate between 50 and 90%^[8]** depending on the conditions of each patient's heart and if any structural heart disease are detected. This success can be classified as **total** (no recurrences of the PVC in the long term) or **partial** (where the recurrences of the PVC have been reduced).

On the other hand, contemporary catheter ablation interventions are highly influenced by the apparition of navigation systems, a novel technology that appeared at the border between the XXth and XXIst ^{[9][10]} centuries. Remote navigation systems allow the characterization and recognition of the cardiac substrates and the measurement of intracavitary signals, represented by local **unipolar and bipolar electrograms**.

These signals are very important for our study, as they have a certain recognizable morphology. In some patients, after the ablation of the PVC, a

modification of this morphology has been detected in the unipolar signal, which has been called the **double negative deflection**. This specific morphology has awakened our interest and will be key to our study.

All things considered, despite the recent advances in technology and even though catheter ablation of PVCs have a high success rate, the apparition of recurrences and the time needed for the whole intervention are issues pending to solve.

At this point is where our study was born, aiming to assess how the procedure of PVC ablation can be optimized.

Hypothesis

We hypothesize that the electrophysiological characterization of different unipolar and bipolar signals detected during the ablation treatment of PVCs can help anticipate the rate of success of the procedure and its effect on the different foci involved on the generation of PVCs

1.1. Objectives

We have based the main objectives of our study in the characterization of different unipolar and bipolar signals, detected on the ablation treatment of PVCs, while assessing the electrophysiological effects that this procedure has had on the different foci that were involved on the generation of PVCs.

Our main goals are:

- To **characterize** the morphology of the unipolar and bipolar signals, measured in the **most precocious isochrone**, during ventricular ablations.
- To evaluate the **precocities** (which are the earliest sites where the depolarization of the ventricle takes place) at the most precocious isochrone and its relation to the outcome of the ablation.
- To judge if the **location** of the most precocious area in ventricular structures can be related to a higher probability of **presenting multiple negative unipolar deflections**.
- To assess if the **detection of multiple negative unipolar deflections** in an intracardiac electrogram has any relation with the **outcome** of the ablation procedure.

1.2. Justification of the project

After the finalization of the study, we will be able to:

1. Assess if the presence of PVCs at certain substructures of the ventricles is related with the apparition of multiple negative unipolar deflections.
2. Evaluate if the detection of double unipolar negative deflections is related to a successful ablation procedure, thus, reducing the amount of time needed for the intervention.
3. Estimate if there is any relation of the precocities, found at each tissue that has been ablated, with the apparition of post-ablation recurrences.
4. Check if specific unipolar and bipolar morphologies and their measured precocities can be associated to particular ventricular structures.

2. Background

2.1. Premature ventricular complexes (PVCs)

Ventricular extrasystoles or Premature Ventricular Complexes (PVCs)^{[3][11]} are a kind of arrhythmia originated at foci found at specific areas of the ventricular tissue. These foci acquire the capacity to generate stimuli at rhythms other than the sinus one. PVCs result in the depolarization, and further contraction, of the ventricle(s) between sinus ("normal") beats causing discomfort in the patient; for example, an irregular or skipped heartbeat followed by a fluttering sensation.

2.1.1. Historical studies

The treatment of ventricular extrasystoles has been studied for a long time. Studies dated as far as 1959 report the resection of ventricular tissue aiming for the excision of ventricular aneurysms, resulting in the elimination of Ventricular Tachycardia (VT)^{[3][7]}.

Before the turn of the millennia^{[9][10]}, **color-coded 3D activation maps** made its first appearance for the characterization of arrhythmogenic substrates. The **CARTO** software for magnetic navigation imaging was also developed at the final stages of the XXth century. Such advances allow actual navigation systems to **merge medical images** that have to be obtained prior to the intervention (such as **Magnetic Resonance Imaging (MRI) or Computed Tomography (CT)**) with 3D mapping. As a result, we obtain more accurate structural information for the characterization of the tissue, MRI can also be used to assess the characteristics of the ablation scar after the procedure, assessing its width and length.

Recently, newer ablation energies, for example electroporation of the substrate, enhancement of the mapping systems and the aim for the control of the

parameters influencing injury formation are some of the principal investigation advances regarding ablation.

Another recent option that has arisen to control scar formation has been the creation of **contact force catheters** that allow the measurement of the electrode-tissue interaction in order to estimate the depth of the injury that is being created.^[21] Contact can be used as a marker of the characteristics of the scar and used as a predictor for future recurrences.^[22]

2.1.2. Clinical implications

PVCs are a **common condition** for people and different cases can be detected without further malignant implications. It is expected that 1 out of every 2 will suffer from occasional PVCs at some moment of their life even if they do not present apparent structural heart diseases^{[4][5][6]}. Moreover, there are groups of people that can be asymptomatic to this condition or even have only isolated episodes with no continuity in time. In fact, PVCs are found between **1-4%** of the general population that undergo short **electrocardiographic recordings** (less than 1 minute) and between **40 and 75%**^[14] of the people wearing a **24-48h holter**.

(Annex 3)

The apparition of PVCs can be influenced by a large number of circumstances that can range from physiological variables up to alcohol, drugs or caffeine consumption.^[15]

PVC treatment is indicated only for “malignant” PVCs, which are those that show these characteristics:^[16]

- **Unifocal PVC:** The depolarization is generated by an only focus.
- PVCs that present an electrophysiological morphology resembling a left bundle branch block.
- **PVCs classified as frequent**, representing a high PVC burden. The threshold for this classification is an amount of 10.000 Ventricular Extrasystoles per day or represent more than the 10-15% of all the daily beats of the patient. (To add some perspective, people with a heart rate of 60 bpm have 86400 beats per day, so 10.000 extra beats would represent an 11.57% of all the beats in a day).
- Certain **ECG morphologies** such as a broader QRS duration than usual (Annex 3) or being detected at specific areas, like the Purkinje fibres or the right/left ventricular outflow tracts.

The importance of malignant PVCs is that they can cause cardiomyopathies or severe ventricular arrhythmias.

2.1.3. Treatment of PVCs

When PVCs are catalogued as **malignant**, treatment is usually indicated.^[17]

There are 2 main paths for their treatment.

Firstly, a **pharmacological treatment is evaluated** with beta-blockers or antyarrhythmic drugs.

If this treatment is not enough to correct the ventricular episodes, a more invasive treatment can be considered: **ablation**.^{[19][18]}

Both of these treatments are done to reduce PVC burden or to treat asymptomatic patients with a reduced Left Ventricular Ejection Fraction (LVEF), which is the volume of blood exiting the ventricles in relation with the volume that enters in every diastole, lower than the 50%.

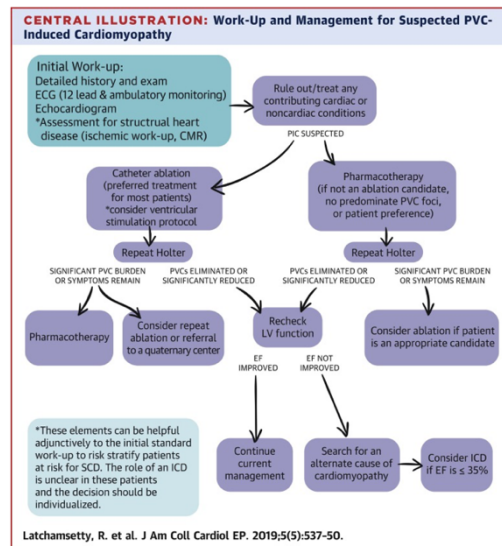


Figure 1. Diagram showing the path followed for PVC evaluation and treatment. Obtained from [6].

Ablation.

This procedure is based on the **introduction of an ablation catheter** inside the patient^{[19][3]}, usually through the groin, in order to access the **internal cavities of the heart**.

Once the catheter is located inside the ventricular chambers, it is guided via intracardiac electrograms to the location that has been identified as the focus of the PVC.

Depending on where the catheter senses the cardiac electric activity, there are 2 different types of electrograms measured:

1. On one hand, **endocardial electrograms**^{[19][20]} allow us to measure electrical activity that is being produced inside the myocardium. This is the approximation that has been used for the electrogram acquisition in the cases that we have studied.
2. On the other hand, **epicardial electrograms** allow us to check the electrical activity from outside of the myocardic tissue, or those areas that are closer to the external surface of the heart. That way, depending on the intensity of the signal recorded, the location of the focus can be assessed.

Finally, when the issue that has been the cause of the arrhythmia has been located, the catheter releases energy from its tip onto the cardiac tissue, aiming to **create a scar**.

Scars are **non-conductive tissue**, so when electric impulses reach the scarred area of the heart they will not be transmitted onto other areas and the arrhythmogenic impulse transmission will be, theoretically, stopped.

The strategy for the generation of the scar differs depending on the type of arrhythmia that is being treated, but almost all of them rely on the creation of lesions or scars on the ventricular walls.

These scars can be made through a wide range of different approaches, each of them represented by the sources of energy used:^[3]

- 1. Microwave energy:** This type of ablation energy uses the oscillation of the molecules inside the tissues to create heat. Ablations done using this procedure result in a uniform, and usually circular, scar that may be more **difficult to control** its width, length and fine morphology. The use of this technique is preferred for **hepatic interventions** rather than cardiac ones.^[20]
- 2. Ultrasound energy:** Energy that causes tissue damage in order to make a transmural scar through the heart walls. This method is still being under study.
- 3. Cryoablation:** The aim of cryoablation is to stop the transmission of the impulse by applying **sources of energy that create cold** to freeze the tissue instead of the use of heat. For example, when treating impulses coming from the pulmonary veins, a **cryoablation balloon** can be used to seal the transmission of the impulse across the veins.
- 4. Transvascular ethanol ablation:** ^[21]
Another technique that was initially used for the treatment of Ventricular Extrasystoles was the transvascular ethanol ablation. This technique is based on the infusion of ethanol in the cardiac substrate in order to create a small infarction of the tissue where the focus is found so that it will not be able to create and/or transmit stimuli generating the arrhythmia. However, this technique has been withdrawn due to the detection of **notable collateral injuries**, such as pericarditis or atrioventricular block, and the apparition of techniques with higher efficacy and fewer complications.

5. Stereotactic radiotherapy: ^[22]

This technique consists of the application of an **X-Ray beam** with a dose of 25 Gy that aims to create a **mixture of nuclear and vascular damage** so that arrhythmogenic behaviour could be reduced.

This technique has fared well in animal models^[23] and, recently, has been used to treat 5 living human arrhythmogenic hearts, reducing the burden caused by PVC.

Regardless, this technique still **needs further studies** to characterize precisely the exact location that will receive the radiation and determine the methodology, as the sample size on human patients is still reduced.

6. Radiofrequency (RF): This source of energy is the **most used for treating PVCs**. It consists of the application of an AC current on the tissue. The power of the energy used in RF ablation is about 35-50W, it causes **heat that can reach up to 90°C**. These temperatures can cause the **denaturalization** of the proteins and cells affected, **necrotization** of the tissue or even **block the tip** of the catheter when intending to reach deeper parts of the endocardial walls.

As a consequence, some RF ablation catheters include a **saline solution** (usually 0.9% saline chloride) that is expelled from the tip of the catheter in order to **lower the temperature** of the tissue. This allows the achievement of **deeper structures** and the creation of a more fluid environment that will, for instance, allow blood flow and avoid blood clot formation on the tip of the catheter.

RF catheter ablation has a success rate between 50 and 90%, resulting in a mean reduction of the PVC burden of 97% and a mean increase of the LVEF of about 10%.

Different energy sources of RF ablation can be used: **unipolar**,^[3] which delivers RF energy between the tip of the catheter and a dispersive electrode patch to avoid creating injuries on other tissues than the one intended, and **bipolar ablation**,^{[3][24]} technique that replaces the dispersive electrode used in unipolar ablation, on the other side of the ablated tissue, with a second ablation catheter in order to create deeper injuries, however, this system is under clinical evaluation.

2.1.4. Applications of RF ablation to PVCs.

Radiofrequency ablation has different modes of application for the different kinds of arrhythmia triggering ventricular mechanisms (Annex 1), but as **PVCs are caused by focal arrhythmias**, (Annex 2) we are going to focus on how PVCs are treated by catheter ablation.

The approach selected for the ablation of focal arrhythmias is the **isolation** of the foci that generate the depolarization.

First of all, when the focus causing malignant PVCs targets to circle the area around the focus/foci that generate the PVC. The isolation of the arrhythmogenic tissue circles the area that is generating the stimuli with non-connective tissue so that the stimuli will not transmit and depolarize the rest of the cardiac chambers, eliminating (or reducing) the incidence of the PVC.

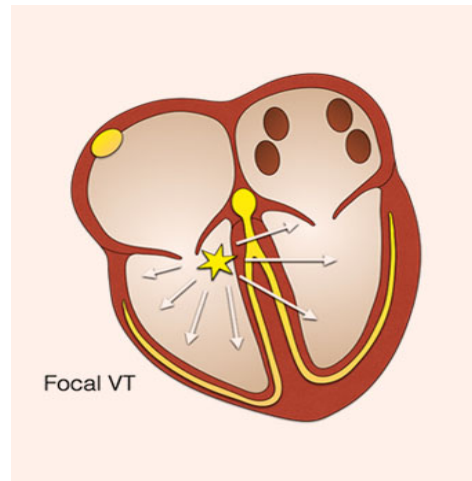


Figure 2. Focus that causes ventricular tachycardia.
Image obtained from [25]

This procedure has a success rate between 70 and 90% and a recurrence rate of 15-25% of the patients [3][26]. There are many different causes for the recurrence of PVCs. Some factors influencing a durable scar and the reduction of future recurrences, are the duration of the energy application, temperature at which the tissue reaches or the contact between the scar and the tissue. All of these variables have a direct effect on the depth, width and durability of the scar that has been created.

On the other hand, catheter ablation rarely presents complications during the intervention. Having only a 2-7% rate of intervention-related complications. The main complications reported in ablation procedures are pericarditis (about 20% of the complications) and the puncture of the walls of the ventricles (around 17%).

Although RF ablation is a technique with high success rate and low complication rate, it does not revert the structural damage that might have been caused by the apparition of malignant PVCs.

2.1.5. PVC innovation

Data about the cause and the variability in PVC generation and propagation are not well known. Recent studies have shown interest in the optimization of the time needed for a correct PVC detection, the actual 24-48h holters provide accurate enough information for the detection of fluctuating PVCs?

Other investigations regarding PVC detection focus on facilitating the detection of PVCs in the general population using electronic devices like smartwatches, with the ability to detect arrhythmias in normal circumstances of life without feeling restrained.^[27]

On the other hand, PVCs found in young, apparently, healthy athletes are considered to be a benign condition, but in time they can turn out to be a major issue that can lead to sudden death. The apparition of PVCs can be related to intense exercise that can even produce dizziness, dyspnoea or presyncope if the intensity of their exercise is not maintained under certain thresholds.^[28]

About the treatment of PVCs, new ablation techniques being investigated are the aforementioned stereotactic radiotherapy and the electroporation technique, that allows the creation of a fast isolation of the arrhythmogenic tissue from the rest of the heart by applying an external electric current that results in the non-thermal isolation of the foci.^[29]

Finally, echocardiography has been used to assess the thickness of the epicardial adipose tissue over time and it can be considered as a biomarker of the outcome of the ablation. It has been seen that the epicardial adipose tissue thickness is higher in patients who have had a failed ablation of their PVCs.^[30]

2.2. Intracavitary electrical signals

The catheters used for these procedures have a set of electrodes that enable the sensing and monitoring of the different electric signals inside the heart chambers. These electrodes allow us to obtain the unipolar and bipolar measurements, which are the main kinds of signals that will be the object of our study.

2.2.1. Unipolar and bipolar signals

First of all, signals are obtained by assessing the differences of magnitude between, at least, 2 separated recordings in a concrete time lapse. **Bipolar signals** can be measured by calculating the voltage differences (over time) between 2 different electrodes located closely.

$$Ve1 - Ve2 = \text{Bipolar signal}$$

Expression 1. Voltage difference between 2 electrodes to calculate the bipolar signal. $Ve1$ for the potential recorded at the 1st electrode and $Ve2$ for the potential recorded at the 2nd electrode.

On the other hand, **unipolar signals** can also be measured. These signals follow the same principle as the bipolar ones (potential difference between 2 recordings).

As a signal is obtained by the comparison of 2 recorded potentials, we need one electrode that will measure the unipolar signal, and another electrode in which the values measured will not affect the unipolar electrode measurements.

Unipolar signals can be achieved by using 2 different techniques.

First of all, we can use what is known as a **Wilson electrode (WCT)**. Which is used as a reference electrode (also used in ECG measurement (Annex 3)), that has a potential equal to 0V^[31]. This potential value is obtained by the combination of the 3 bipolar leads of an ECG (I, II, III).

The other technique that can be used to obtain unipolar signals is also based on the use of a reference electrode. But, in this case this reference uses an electrode located far from the measuring one (ideally this separation between electrodes would be infinite) so that its potential recording can be approximately zero. This far away electrode can be located on the same ablation catheter, or on other catheters (reference catheter).

After assuming that the potential obtained from these 2 references equal to zero, we obtain the unipolar signal by calculating the difference of potential measured by the unipolar electrode and the WCT.

$$V_{unipolar} - WCT(0V) = Unipolar\ signal$$

Expression 2. Calculation of the unipolar signal. Measurement of an electrode – 0.

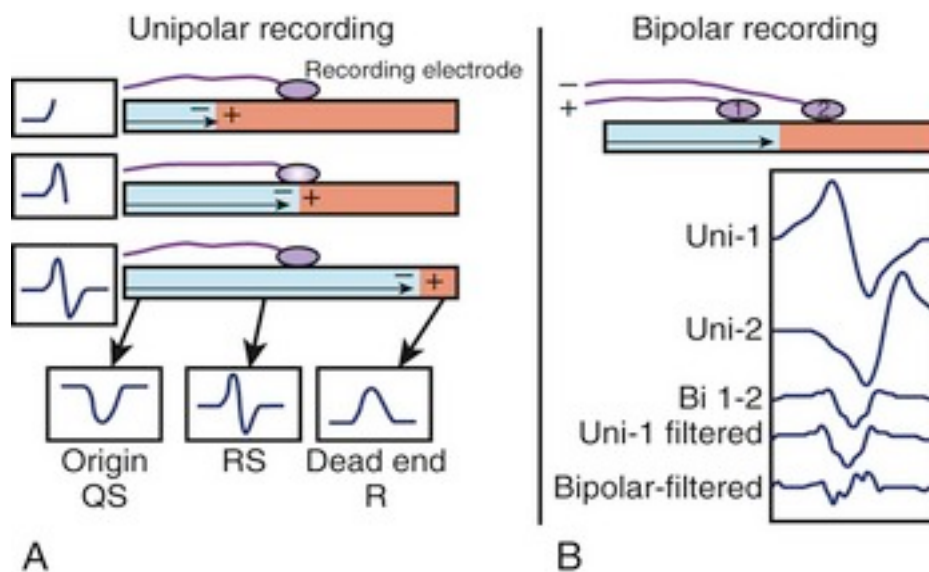


Figure 3. Unipolar measurement of a depolarization (left) and bipolar measuring of the differences between electrodes (e1 and e2) (right). Image obtained from ^[32]

As we can see in figure 3, unipolar signals have a defined morphology where we can firstly find an increase in voltage followed by a pronounced decrease in tension, what we will call the unipolar negative deflection. This concrete part of the unipolar signal will be very important for our study. Observationally, it has been seen during the ablation interventions that this morphology can change, presenting multiple negative deflections (usually 2, but in some cases even more), along the extent of the unipolar signal. Depending on how many drops can be seen in the unipolar electrogram, **before it reaches its lowest peak.**

This morphology is called a double negative deflection, triple negative deflection, and so on.

From the point where the unipolar signal starts to become positive, if any drops are observed they are not taken into account, as they might be the result of measurement artefacts.

Electrophysiological signal morphology is associated with the directionality of the wave respect to the electrode.

If the activation wavefront is approaching the measuring electrode, it will be located in the positive part of the potential field, thus, resulting in a positive deflection, an increase, of the detected signal.

On the other hand, if the wavefront has already gone through the location of the measuring electrode, it will be located on the negative part of the potential field of the sensor, resulting in a negative deflection of the signal, resulting in the voltage decrease of the electrogram. [33]

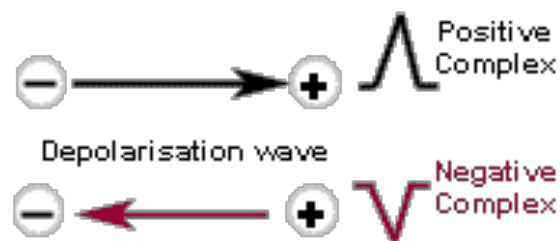


Figure 4. Representation of waves detected by an electrode dependent on their direction of transmission. Image obtained from [34]

In the unipolar and bipolar electrograms, if the incoming signal has been generated by the myocardial cells directly located underneath the electrode, it is called a **local electrogram**. If the stimulus has been generated by myocardial cells that are located further away it is called a **remote electrogram**. The deflections of the unipolar and bipolar signals can be used complementarily to judge whether a measured electrogram is local or remote. These electrophysiological measurement principles are also used for measuring the electrical signal of each of the 12 electrodes/leads of an ECG (Annex 1).

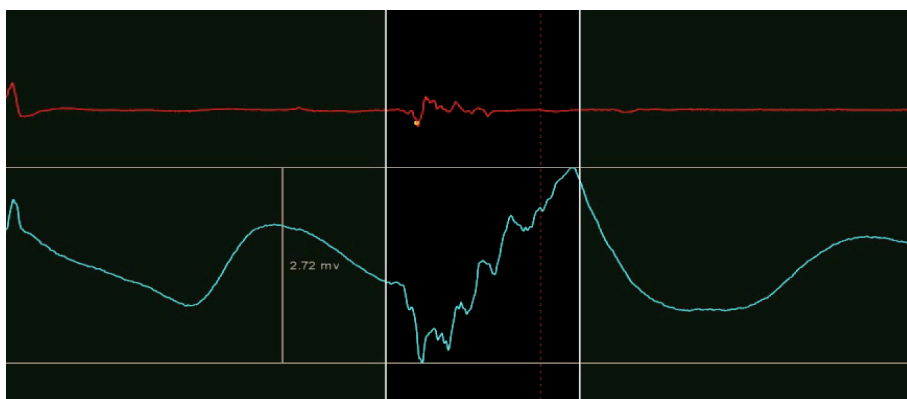


Figure 5. In this figure we can see a bipolar recording of low amplitude (top). And a unipolar signal presenting a double drop (bottom). It can also be seen the voltage caliper used for calculating the voltage of the signals studied.

2.2.2. Intracavitary signals characteristics

As unipolar and bipolar electrograms differ in their acquisition, they also give us different information that can be used complementarily to identify the characteristics of the ventricular substrate.

First of all, as **unipolar electrograms** are obtained by an only electrode (compared to the reference electrode), its morphology is indifferent from the directionality of the passing wavefront. Nevertheless, these electrograms are sensitive to far-field potentials, for example a common source of noise is the one located at 50 Hz introduced due to the use of electrical devices, which can add noise into the measured signals.

These electrograms are affected by the distance between the sensed point and the measuring electrode, lowering the amplitude of the unipolar signal and the distance between its positive and negative peaks.

For unhealthy myocardium, only the negative part of the unipolar signal is due to the cells directly located underneath the measuring electrode, local electrogram.

For **bipolar electrograms**, these characteristics change. As the signal is obtained by comparing the unipolar signals obtained at 2 different electrodes, the values measured are dependent of the directionality of the incoming stimuli. These electrograms are also less sensitive to far-field interferences and are helpful for the evaluation on if the measured signal is local or remote.

2.3. PVC mapping

2.3.1. Navigation systems

Whenever a PVC is produced, it is important to characterize its morphology and assess where it is taking place.

Classically, the approach to locate the ablation catheter during the interventions was by using a fluoroscopy (RX) arch to ensure the correct location of the catheter during the intervention. Nevertheless, the fact the intracardial electrograms give us information about the local activation can be used as a way to control the location of the ablation catheter at a given moment in time.

The acquisition of electrogram information has been the main cause of the emerging of the **navigation systems**. Navigation systems aim for the characterization of the arrhythmogenic substrate and the location and characterization of the area of the tissue that causes the arrhythmia, all of these while allowing the location of the catheter in real time. They allow the detection of points of interest (that may be interesting due to precocities or structural information) and annotate them in 3D anatomical, color-coded maps.

There are 2 main types of navigation systems; impedance-based and magnetic-based. ^[35]

1. Impedance-based navigation systems: ^{[36][37]}

Impedance (Z) is the opposition that a tissue presents to an AC current when a voltage is applied.

Impedance-based navigation systems use that principle to characterize cardiac tissues prior to an ablation procedure, that way, the differences of impedance that are measured at each point help the assessment of the state in which the tissues are.

Studies have shown that for injured or non-conductive tissues (such as scars) the characteristics of the affected tissues are modified, and the impedance measurements decrease. whenever voltage is applied.

For PVC characterization using impedance mapping there are several aspects to take into account. Firstly, a low amplitude AC current is generated, with a frequency in the range of kHz, across the thoracic cavity of the patient, thus, generating **impedance**. Depending on the position at which that current is being measured, different voltage gradients are detected.

The measurement of voltage gradients depends on the use of an even number of perpendicularly placed electrodes. If 2 electrodes are placed orthogonally on the skin of the patient and a sensing element (in our case the ablation catheter with the electrodes on its tip) is placed among them, while they are under the influence of the electric field, we can detect differences in voltage caused by the catheter being closer to one electrode or the other. Measuring the voltage gradient among both of them. They are assumed to be located equidistantly.

In impedance-based navigation, 3 pairs orthogonal patches (known as skin electrodes) are placed on the skin of the patient. Then, the impedance catheter is placed in the endocardium of the patient and a non-stimulatory current generates an electric field.

Then, the transthoracic impedance is measured by assessing voltage gradient variations between the tip of the catheter (inside the patient) and each of the pairs of the skin electrodes.

However, this technique faces some limitations. As impedances assess differences between the endocardium and skin potentials, the measurements of one patient cannot be compared to the readout of another one due to interpatient variability.

Even the impedance navigation measurements observed in the same person may differ in time, causing non-linear results. For example, measurements acquired at an equidistant location between 2 skin patches, may not result in constant differences in impedance. Mainly due to the non-symmetry of the internal cavities of a patient or due to its variations over time (such as the air in the lungs resulting from breathing patterns), which will cause impedance disparities

2. Magnetic-based navigation systems: [36-39]

Magnetic-based navigation systems rely on the use of magnetic fields for the mapping of the heart.

Remote magnetic navigation (RMN) is based on the use of three magnetic generators, located underneath the operating table, that generate a magnetic field (B_0) around $5 \cdot 10^{-5}$ and $5 \cdot 10^{-6}$ Tesla (T) [40] (to give a little insight, the magnetic field of the earth is about $3 \cdot 10^{-5}$ T, and the magnetic field of a magnetic resonance scan ranges between 1.5 and 7.5T).

This magnetic field is oriented at a certain direction that can be modified at operator criteria depending on the direction wanted at each given time. The field is complimented by a magnetic ablation catheter that has 3 magnets and a sensing element on its tip, so that the catheter will be aligned parallelly to the external magnetic field.

The three magnets of the catheter and the three magnetic fields that are being generated, allow the triangulation of the position of the catheter respective to each one of them.

As the catheter moves along the endocardial cavities, local electrical activation can cause small, measurable, deflections on the catheter tip that can be used to recreate the local three-dimensional morphology of the heart and the activation patterns found in the heart so that we can assess at which spots larger precocities are measured.

This technique achieves a higher stability of the catheter during the intervention, easing the use of RF energy and control over the scar. It also reduces measuring differences caused by physiological variations or patient variability.

Currently, there are 3 main companies that commercialize navigation systems

1. Ensite (Abbott) [41]

Ensite are a group of commercialized navigation systems, mainly impedance-based. There are 2 main EnSite navigation systems.

Firstly, the EnSite Velocity navigation system is based on impedance field technology to detect changes in different tissues, working at a sampling rate of 8136 kHz. Then, the EnSite Precision mapping system uses mixed navigation (impedance and magnetic) in order to lower the usual limitations faced by the use of impedance-based navigation systems, working at a sampling rate of 5.6 kHz.

The catheter used in these navigation systems have multiple electrode poles that allow them to detect different anatomical points and annotate them on a pre-acquired chamber anatomy.

2. Rhythmia (Boston Scientific) ^[42]

Rhythmia is another device for the 3D mapping of the cardiac chambers in real-time. It uses a hybrid mapping system combining impedance-based navigation, if a more flexible approach is aimed, and RMN, maximizing the efficiency of the ablation while obtaining 3D maps in a really small amount of time.

3. CARTO (Biosense Webster)

This Remote Magnetic Navigation System is one of the most widespread for the mapping and characterization of arrhythmogenic substrates. CARTO combines magnetic location and current-based visualization of the data to provide catheter tip and curve visualization in order to give accurate catheter information and readouts in real-time^[43].

The catheters used by the CARTO software have a sensing tip composed by 3 magnets that allows its location.

This sensing tip has 6 degrees of freedom, and its position is expressed in terms of the (x,y,z) spatial coordinates RPY notation for orientation and rotation of elements in a 3D. (Annex explicació RPY). These catheters allow the **reconstruction of the cardiac cavities** while creating a colour coded map that sets its starting point as the most precocious activation detected (in red) up to the point that is closer to the sinus rhythm (in purple).

2.3.1. Activation mapping

Activation mapping is a valuable strategy when trying to locate the origin of Ventricular Extrasystoles. These maps are obtained through the recording of local electrograms on multiple sites of the heart.

The result of this technique is the obtention of three-dimensional, color-coded maps known as **activation maps**. For the **CARTO** software, these maps are coloured in a palette ranging from red to purple depending on the measurement of the earliest activation points. Meaning that those annotated points showing the earliest electrical activation respect the sinus beat (the ones presenting larger precocities), will be red-coloured, whereas points presenting smaller precocities will be yellow-coloured and so on up to the points presenting activation closer in time to the sinus beat that will be purple-coloured.

These colours are used to define isochrones. Isochrones are areas that present the same value of their magnitude across all of their extension. In our study, isochrones will be used to define areas in which the precocities found will have the same colour for similar values.



Figure 6. CARTO colour-coding of the map depending on its precocities.

Another important aspect of activation mapping is that whenever a point is considered to be of interest for future studies, its electrophysiological (unipolar/bipolar signals and the signals recorded by the 12-lead ECG) and location information can be annotated on the 3D map, the exact location of that point of interest is saved so that the ablation catheter can return to that exact same point for further study.

The characterization of the substrate and location of the foci on the operating room strongly depends on the apparition of PVCs during the mapping. If the conditions for PVC characterization are not met satisfyingly during a certain lapse of time, the heart can be stimulated artificially at different sites in order to recreate the morphology of the PVC and detect which stimulated morphology resembles the most to the patient "PVC template". This technique is called **PACE-MAP**.

The CARTO software allows us to compare the signals obtained during the stimulation of the different areas of the heart with the patients' detected PVCs. That way, accurate activation maps can be obtained, and the focus of the PVC can be located (due to the similarities among the signals detected at the stimulated areas and the PVC).

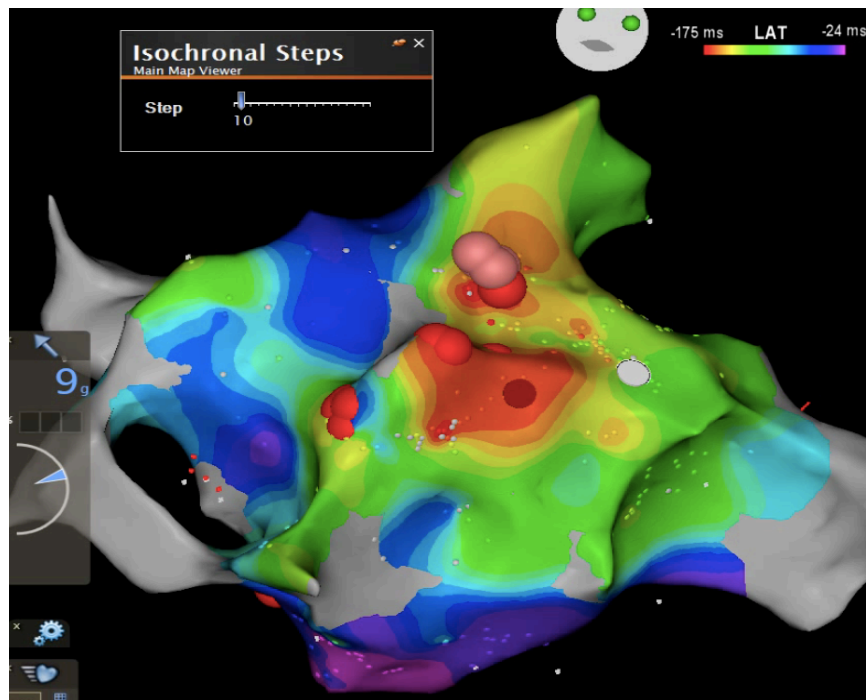


Figure 7. 3D activation map showing the direction of the depolarization following the colour palette described. Red for the earliest activation point up to purple.

2.3.2. Catheters used in CARTO mapping.

Biosense Webster has developed a set of catheters that are useful for the characterization of the ventricular substrate using magnetic navigation. These catheters are compatible with the CARTO software and the mapping data that they have recorded is displayed on the operator interface.

The two main catheters that are used for the mapping and treatment of PVCs using CARTO are:

1. **SmartTouch:** This is a contact force catheter that can display the parameters obtained during the ablation, such as power, impedance, stability, average force of the contact or location, on the CARTO interface. This contact sensing of this catheter is done using the 3 main parts of its tip. ^{[44][45]}

First of all, we can find a transmitter coil, which is used to send location reference signal. Then, the movements of the coil are detected by a location sensor and, finally, a precision spring is used to deliver movement in response to the contact force. All this information is also shown on the interface, where a vector points at the direction of the tip. The tip is also colour coded, changing its colour as the targeted force is approached.

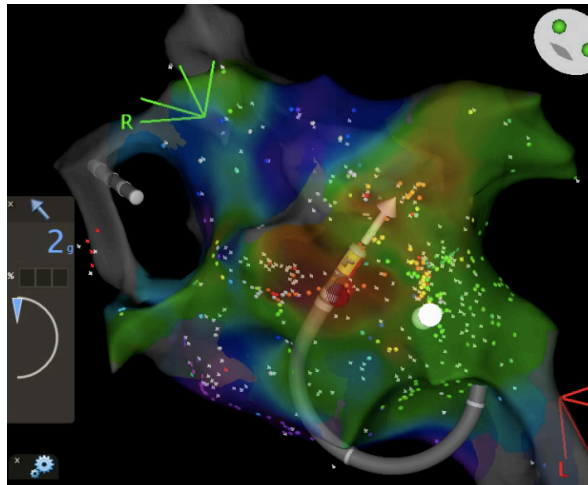


Figure 8. Smart Touch catheter used in the ablation of a PVC where the directionality of the tip is shown.

2. **Pentaray:** This catheter, also developed to be compatible with the CARTO interface, made its appearance in 2012.^[46] The Pentaray catheter is **only used for the mapping** of ventricular substrates and not to ablate them.

It is composed by five soft flexible branches that allow the approximation of the catheter to difficult surfaces, avoiding getting stuck on, for example, the mitral valve. These branches are present as much as 20 poles that allow the sampling of multiple points simultaneously (inter-electrode distance of 1mm).

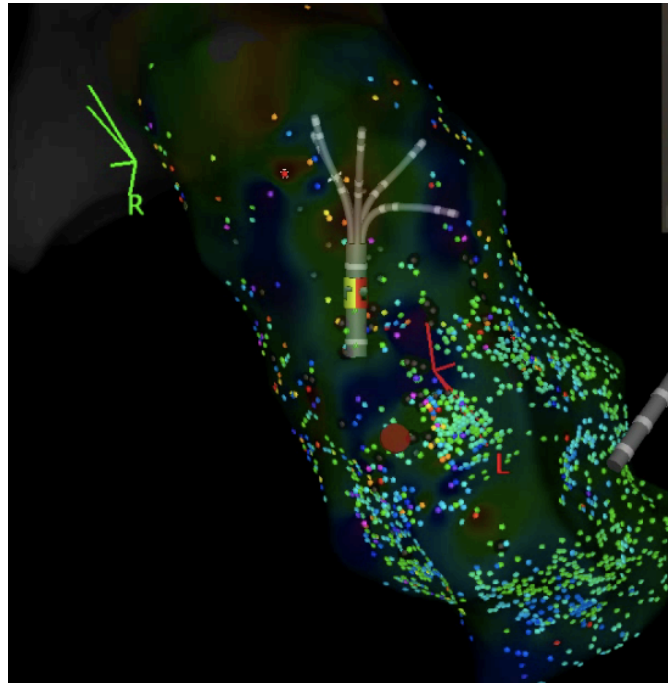


Figure 9. Use of the Pentaray catheter for the treatment of a PVC. We can see the 5 flexible legs that are used for mapping the substrate.

2.3.3. State of the situation

This project has been developed) in the Arrhythmia Unit of the Hospital Clínic of Barcelona.

This unit has the conducts, regularly, several cardiac electrophysiological studies and interventions aiming to upgrade the quality of life of people in need of their services.

Relating to our study, in the Arrhythmia Unit patients diagnosed with PVCs that do not respond to pharmacological treatment are treated through RF cardiac ablation, which is a fairly more invasive procedure aiming to eliminate (or reduce) the PVC burden and future recurrences (which are the re-appearance of PVCs posterior to their treatment). More precisely, 24 cases of PVC patients have been treated using remote magnetic navigation systems to guide the ablation since 2019 that resulted in the total 34 PVC cases that have been studied, as some patients presented multiple PVCs.

In this Unit there are 2 operating rooms for the treatment of different electrophysiological conditions, software that fits the requirements needed for electroanatomical mapping. We focused on the use of the software CARTO for remote magnetic navigation (and the specific magnetic catheters needed). And other devices used during the intervention, for instance, cardiac stimulators for pacing and polygraphy systems for the monitoring of intrinsic cardiac signals.

Nowadays, research studies involving catheter ablation are searching for alternatives that result in the **reduction of the extent of the procedure**, new techniques, such as electroporation, are being studied in order to

reduce the amount of time needed in the intervention and the **reduction of the apparition of recurrences** at some point after the ablation. Contact force catheters are being used to have a more direct control on the creation of the injury and its width.

3. Market analysis

Currently, the study of the cardiac intracavitary signals has arisen interest due to the possibility of extracting information about the state in which the cardiac tissue is during, and after, the ablation.

That idea is being developed by several study groups that are assessing how the unipolar electrograms measured during an ablation can be used to find the origin of the stimuli responsible for the PVC by checking the morphology of the unipolar signal detected at the site of earliest activation.^[40]

Other studies have assessed the relation of the unipolar electrograms to evaluate if its morphology is affected by RF characteristics of the procedure, such as if high-power or conventional-power RF ablation is used (Ejima et al. 2019),^[48] during the intervention.

But the morphology of unipolar electrograms has been used to guide interventions. These morphologies can also be used as markers of the outcome of the ablation^[47] (Huang et al. December 2020), depending on the variation detected on the electrograms during the ablation.

For example, the elimination of the unipolar negative deflection^[49] (Ejima et al. 2020) has been related to causing transmural necrosis and the irreversibility^{[50][51]} of cardiac diseases (de Bakker et al. 2019).

As unipolar electrograms give information of the near-field of the cardiac tissue, their study is very promising for future characterizations of the cardiac substrate.

Their use can be helpful for localizing the foci that generate the PVC and provide information of the reversibility of the cardiac disease.

When recognizing a certain morphology, the success of the intervention can be evaluated, thus, potentially leading to a reduction of the time used for treating these diseases and the decrease of future PVC recurrences.

4. Conception engineering

4.1. Talking points

There are several different approaches that can be evaluated when characterizing PVCs. In this section, different strategies are going to be discussed and, finally, the strategy chosen will be introduced.

There will be three main talking points that influence the study and the general outcome obtained; firstly, we will talk about the **source of ablation energy**, then, **navigation systems** that can be used will be discussed. And, finally, the **study of the points** taken will also be under consideration.

Having examined all of these options, the final strategy for the development of our study will be structured.

4.2. Possible solutions

1. Sources of ablation:

There are many sources of ablation that can be used for ventricular substrate ablation, but here, we are only going to compare the two techniques that are mostly used, them being RF ablation and cryoablation.

First of all, RF ablation is used for reaching deep structures of the cardiac tissue while having a high efficacy and low recurrence rate. Nevertheless, concerns have been raised over tissue heating and scar depth.

On the other hand, cryoablation can be used to create larger, but narrower, scars which also take longer time to develop and present a higher recurrence rate than those done using RF. However, as cryoablation catheters adhere to the surface of ablation, they can be useful for accessing areas of great mobility, such as the papillary muscles.

2. Navigation Systems

a. Magnetic navigation mapping: As magnetic navigation has already been mentioned, we will focus on how its use can benefit the purpose of our investigation. Firstly, the use of external magnets and the magnetic catheter allows a more precise location of the catheter once it is inside the patient without the need of using fluoroscopy, thus, reducing the exposure to ionizing radiation.

It also enables the reconstruction of the cardiac cavities and the building of the geometry of the patient following the movement of the catheter along the cardiac cavities. This reconstruction is complemented by the possibility to tag the information of local areas of interest by annotating points on the generated map.

The most common software for magnetic navigation is CARTO (Biosense Webster). However, this software has limited application when the mapping catheter has not been manufactured by Biosense Webster.

b. Impedance-based mapping: Impedance-based mapping measures local currents taking place among 6 orthogonal patches located on the skin of the patient while being subjected to an electric field.

On one hand, this type of cardiac mapping allows the simultaneous pacing and ablation of the substrate and the compensation of distortions produced by the breath or other movements of the patient.

On the other hand, this technique needs of intracardiac reference (which is provided by another catheter that cannot be moved) and it is subjected distortions caused by inter and intra-patient variability and electric field distortions.

The most common software for magnetic navigation is NAVx (EnSite). NAVx is an open system, meaning that it allows the visualization of the navigation whether it is by using catheters manufactured by EnSite or those which have been made by other manufacturers.

c. Joint mapping: Finally, a novel high resolution mapping system is the RHYTHMIA system. It combines technology from both magnetic and impedance-based navigation for 3D mapping.

It allows a faster obtention of the map[] and a higher signal to noise ratio of the final image (which is acquired by reducing the influence of the far-field while enhancing near-field potentials, all in all allows a better measurements of those areas closer to the point that is being measured without being as affected by potentials that are located further away). Nevertheless, in order to use benefit from the use of impedance-based mapping, an electroanatomical map created through magnetic mapping has to be made in advance.

3. Study of the annotated points:

Once the mapping technique and the source of energy have been discussed, we will focus on the different approaches that can be assessed for studying the characteristics of the points annotated on the 3D map. We have envisaged 3 different approaches to the study of the data.

The maps of our study had a large number of annotated point, having an average value of 488.41 points per PVC map.

The first issue that had to be assessed was if all of the points had to be taken into account or just the ones present in some specific locations.

One of the options that were contemplated was delimiting the tissue in different isochrones, classed by their precocities, and assessing a set of points with presenting the earliest electrical activation on each isochrone.

The last option evaluated was to characterize the most precocious isochrone (extension and location) and study only the 10 most premature points of that area.

4.3. Proposed solution:

Overall, having gone through the different alternatives that might have an influence on the outcome of our study, the chosen solution consists of:

- Use of Magnetic Navigation mapping systems, provided by the CARTO software that will let us obtain color-coded activation mapping, annotate points of interest on the three-dimensional map and locate precisely the catheter in real time and get the electrophysiological information at specific points of the ventricles.
- Use of RF ablation for the treatment of PVCs due to its higher efficacy and lower recurrence rate.
- Characterize the **most precocious isochrone** and the **10 most premature points found there**.
- Study the electrogram morphologies of the points evaluated and judge if the ablation intervention had caused significant variations on its morphologies that can be used as biomarkers for prediction of its success.

5. Detailed engineering

This section is key for the understanding of how the project was carried on. Here, detailed information of the materials used for the characterization of the electrograms, the different steps that were done for the study of the morphology of the signals and the results obtained is going to be explained.

The information of this section is divided in materials, methods, results and discussion.

5.1. Materials

The material used for the development of the project have been:

1. A hard disk containing the maps obtained using CARTO while the ablation of PVCs was taking place. In those maps, there were specified the data of the ablation points, the annotated point for the recording of the unipolar and bipolar electrograms, the location-annotated points, the most precocious points and the total number of points that the map contained.
2. The CARTO software running on a Windows computer.
3. SPSS software for the recording of the electrogram measurements on the database and their posterior statistical analysis.

5.2. Methods

5.2.1. Overview

The main aspects of the process followed for obtaining the data of the electrograms is shown in the diagram represented in the Figure 10.

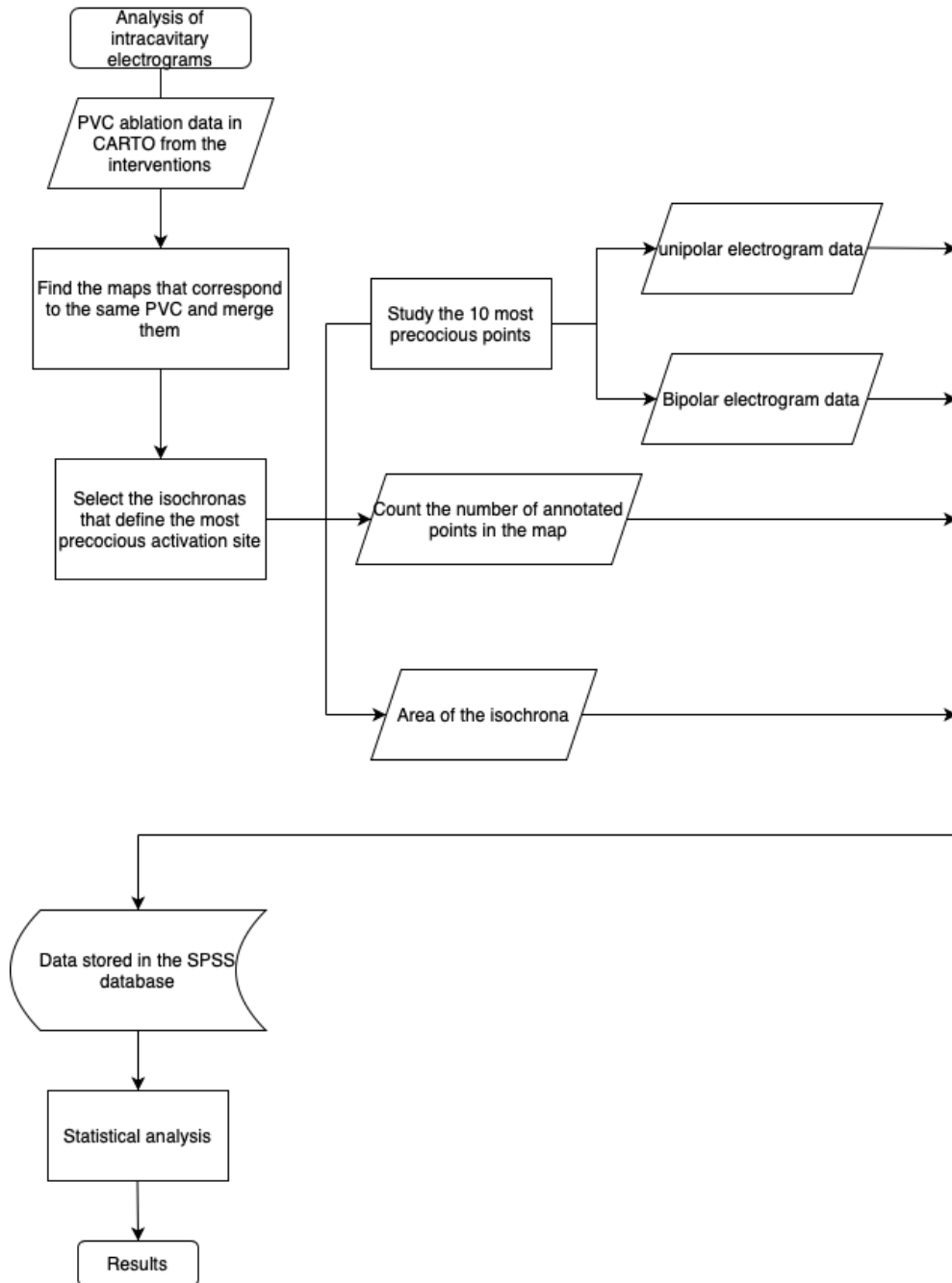


Figure 10. Flowchart of the steps taken for the evaluation of the points annotated in the PVC maps and their electrograms.

5.2.2. Segmentation of the maps

For the classification of the results, we have decided to group the structures were PVCs originated in 5: the left ventricle (LV), the right ventricle (RV), the summit, the pulmonary artery (PA) and the cusps of the aorta.

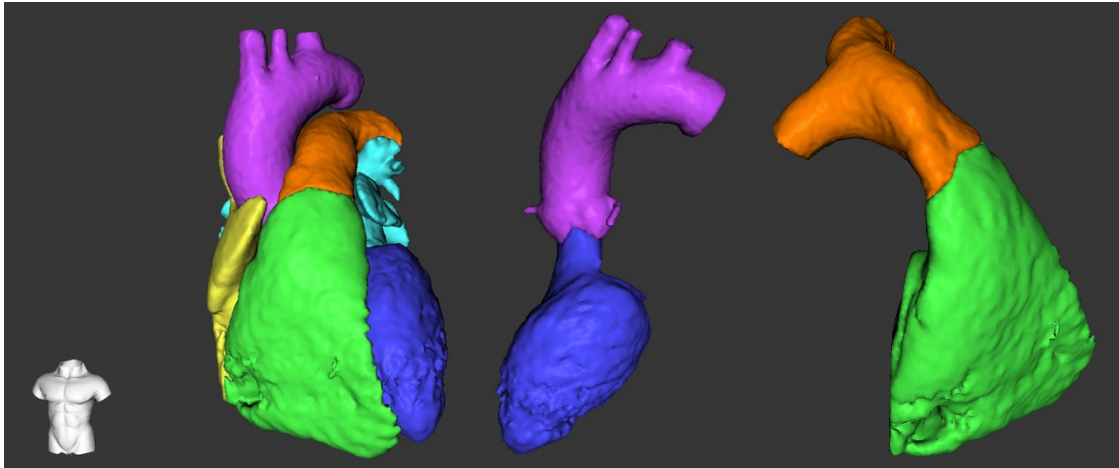


Figure 11. A) Anterior view of the heart as a whole. B) View of the LV (blue) and its connexion with the aorta (purple) through the cusps. C) View of the RV (green) with the pulmonary artery (orange).

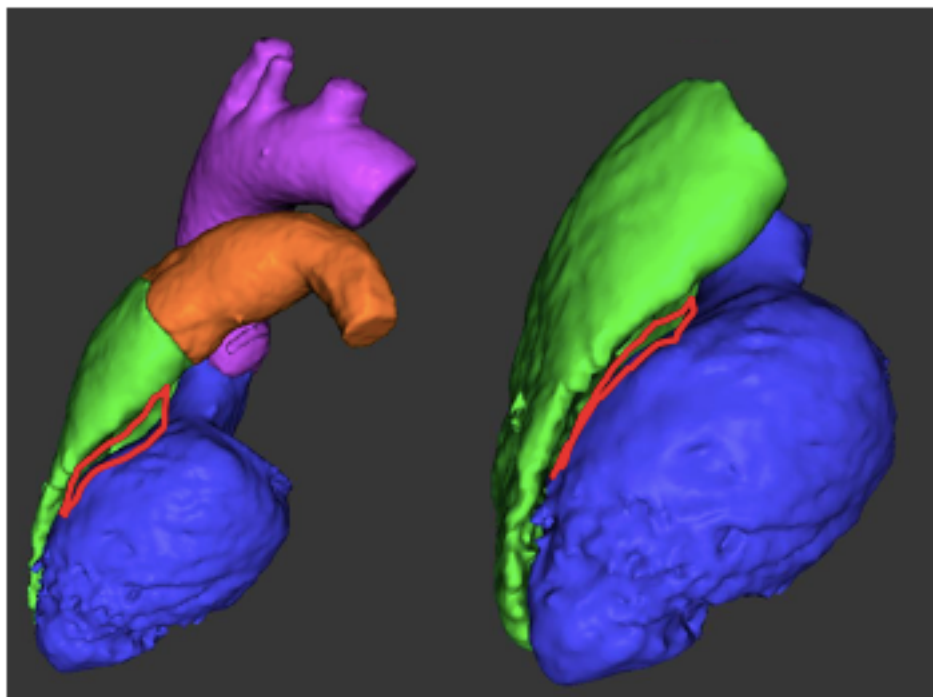


Figure 12. View of the 5 areas studied (left) and both ventricles (right) with the summit marked in red.

5.2.3. Map processing

The first step for the classification of the PVCs of each patient, was to assess the electrocardiographic signal morphology of the PVC(s) obtained for a single patient.

If the morphology of the PVC electrograms was similar enough between different maps recorded for a patient, those maps would be merged into a new, single, map containing all the points from the same PVC morphology. Else, if the PVC electrogram morphology differed, it would be considered as an origin for a different PVC. That way if a patient had multiple PVCs, different activation maps would be created depending on the number different PVCs detected.

Once the maps had been merged, we counted the number of points present in the final map and performed an isochronal classification of the map. Meaning that we delimited the ventricular tissue in different areas to measure the extension of the most precocious area depending on their precocities. The step used to define the isochrone was equal to 10.

Finally, the CARTO software also allowed us to confirm which catheter was used during the ablation, either if it was the SmartTouch or the Pentaray.

The maps belonging to each patient were saved in a backup hard disk for their further evaluation with CARTO.

This process was repeated for each patient and their respective PVC(s).

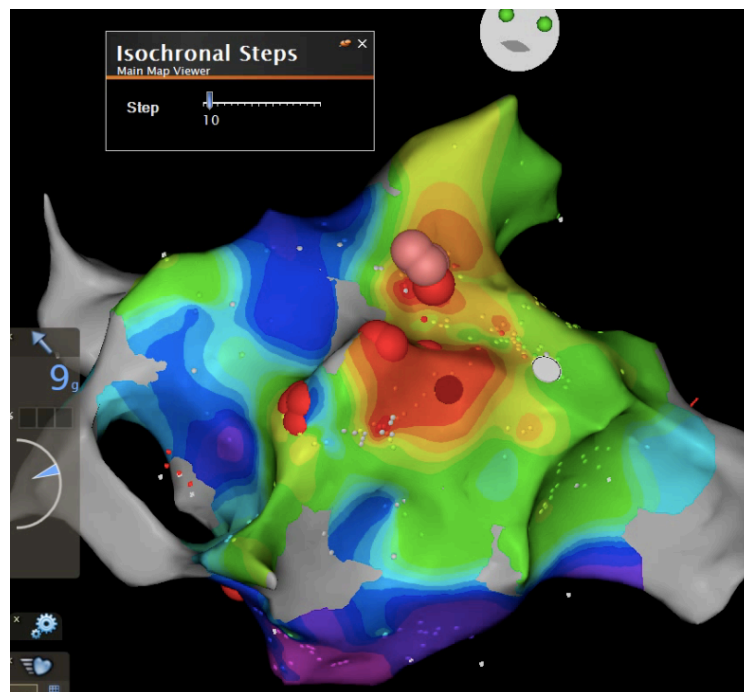


Figure 13. 3D activation map showing the tissue divided in 10-step isochronal maps.

5.2.4. Study of the points

After the map work was finished, we proceeded to study the electrograms of the points causing the PVC.

For the selection of the points, they were sorted by their earliest activation using the CARTO category called LAT (Latest Activation Time). The points selected were the 10 most precocious points of each map, considering the smallest LAT (the most negative one) to be the earliest activation time.

The selection of the most precocious point was also interesting to judge which specific area of the ventricles was the one causing the PVC.

	⬆	LAT	Elect.	CL	F...	PASO™	Tag	Type	Time	Comment
254	●	-162	MAP ...	763	7				11:18:13	
222	●	-159	MAP ...	790	1				10:59:00	
255	●	-158	MAP ...	750	6				11:18:19	
52	●	-154	MAP ...	701	9		LO	Loca...	10:30:46	
76	●	-149	MAP ...	739	1				10:34:02	
79	●	-149	MAP ...	752	1				10:34:31	
83	●	-149	MAP ...	767	0				10:35:41	
86	●	-149	MAP ...	780	1				10:35:55	
256	●	-149	MAP ...	738	6				11:18:20	
265	●	-149	MAP ...	727	5				11:19:45	

Figure 14. Example of a CARTO point list to sort the maps depending on their LAT. Note that the highlighted point has a LO tag. It means that that point only gives structural information and its electrophysiological information should not be taken into account.

At this point, we have the map for a particular PVC with the isochrone of the earliest activation and the list of the 10 most precocious activation points selected. It is now when we proceed to the electrogram analysis of each point.

First of all, we visualized the ECG signals of the point by displaying all the signals corresponding to each lead of the ECG, plus the unipolar and bipolar electrograms.

The ECG derivations were used to determine the initial activation of the QRS (Annex electrofisiologia), that determines the ventricular systole. That initial QRS activation is the one that we will compare with the unipolar and bipolar signals to measure their precocities.

For the bipolar signals, **the precocity in relation the QRS activation and their amplitude (in mV) was measured.**

On the other hand, for the unipolar signals we measured:

1. Their precocity in relation to the QRS.
2. The amplitude of the unipolar signal (in mV).
3. The amount of time between the initial activation of the unipolar signal and the peak of the negative deflection, which we called the negative precocity.
4. The number of unipolar drops.
5. The amplitude of the unipolar negative drop (in mV).

These measurements were done using the Voltage and Time Caliper functionalities available for measurement of time and potential variables. They were performed for each of the 30 PVC maps.

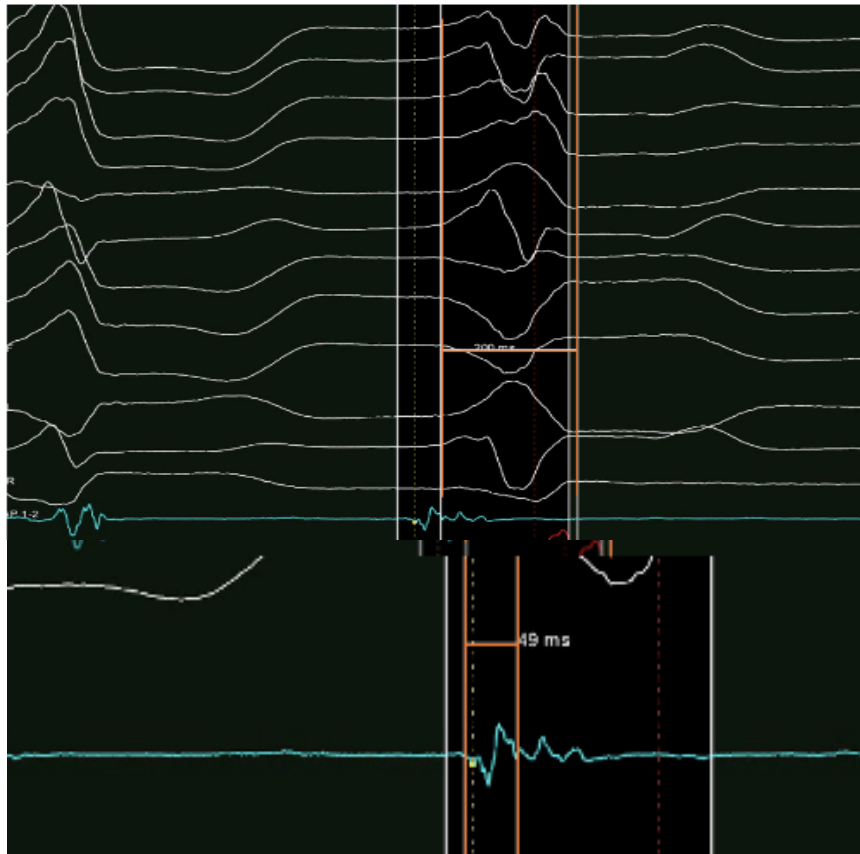


Figure 15. Time caliper resulted in orange. At the top figure, its left margin has been set at the origin of the QRS. On the bottom figure, the right margin of the caliper has been moved to measure the bipolar precocity at this point.

5.2.5. Use of SPSS

The results of the quantification of the electrograms were recorded in a database running on the SPSS software.

With the data of the unipolar signals, we proceeded to calculate the slope of the unipolar drop and the fraction of the unipolar signal amplitude that corresponded to the drop, using the relation of the two variables.

Finally, after all the data had been recorded and transferred into the database, a statistical analysis was performed to judge the relationship of the detection of multiple unipolar drops with the outcome of the procedure.

5.3. Results

The results obtained for this study were obtained by performing a Tukey's method comparison, on R Studio, of the variables studied for the different ventricular areas studied. These were the Right Ventricle (VD), the Left Ventricle (VI), the cusps (CUSPIDES), and the Summit (Annex 6).

For the evaluation of the results unipolar signals that were excessively noisy where unipolar negative deflection could not be assessed were given a 0.

5.3.1. Bipolar signals.

First of all, for the bipolar signal, the locations evaluated showed mean precocities of 30.86ms before the initial activation of the QRS, with the most precocious areas being the summit (43.3ms) and the right ventricle (33ms). (Table 1 and Figure 16).

ISOCORONA_loc1	emmean	SE	df	lower.CL	upper.CL
VD	33.0	2.22	259	28.6	37.4
VI	24.4	2.22	259	20.0	28.8
CUSPIDES	26.6	2.48	259	21.7	31.5
AP	27.0	4.45	259	18.2	35.8
summit	43.3	4.45	259	34.5	52.1

Table 1. Mean bipolar precocity at each isochrone observed. It is also stated the standard error (SE) for each variable and the upper and lower confidence levels (CL). Which show the range in which the bipolar precocities will be found in the 95% of cases (CL = 95%).

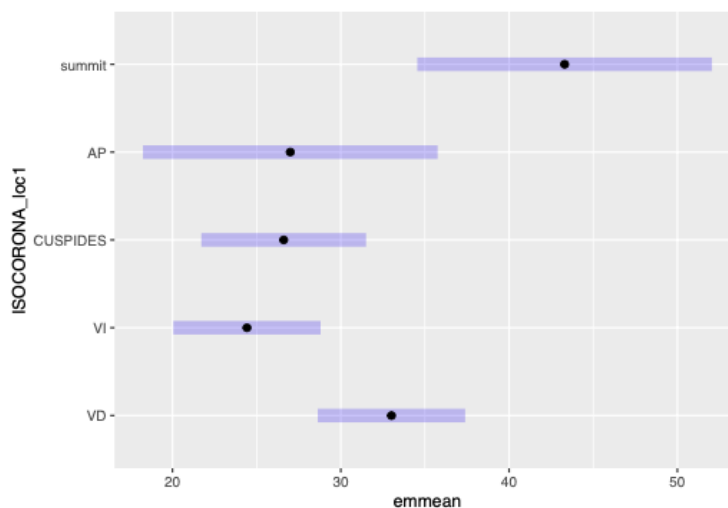


Figure 16. Plot showing the confidence interval where larger bipolar precocities can be found at CL = 95%.

We contrasted the means among the different areas, and we obtained that the differences in bipolar precocities were significant between the left ventricle and the summit (24.4 +- 2.22 vs 43.3 +- 4.45, $p = 0.0017$) and between the cusps and the summit (26.6 +- 2.48 vs 43.3 +- 4.45, $p = 0.104$). However, the comparison of the right ventricular and left ventricular activations resulted in a p -value of

0.052, so we decided to further investigate the relationship of the precocities of these two areas by comparing their unipolar signal precocities

contrast	estimate	SE	df	t.ratio	p.value
VD - VI	8.588	3.14	259	2.732	0.0520
VD - CUSPIDES	6.403	3.33	259	1.921	0.3090
VD - AP	6.013	4.97	259	1.210	0.7457
VD - summit	-10.287	4.97	259	-2.070	0.2363
VI - CUSPIDES	-2.184	3.33	259	-0.655	0.9655
VI - AP	-2.575	4.97	259	-0.518	0.9855
VI - summit	-18.875	4.97	259	-3.798	0.0017
CUSPIDES - AP	-0.391	5.09	259	-0.077	1.0000
CUSPIDES - summit	-16.691	5.09	259	-3.277	0.0104
AP - summit	-16.300	6.29	259	-2.593	0.0746

Table 2. Comparison of the mean bipolar precocities for the assessment of signification.

The mean bipolar amplitude por all the isochrones studied was 1.9mV. The left ventricular signal was the one presenting the largest bipolar amplitude (5.656 +- 1.24 mV) with the lowest amplitude being measured in the summit (0.261 +- 2.49 mV) but no significant statistical differences could be found between the different structures observed (table 3 and figure 17).

ISOCORONA_loc1	emmean	SE	df	lower.CL	upper.CL
VD	1.550	1.24	259	-0.899	4.00
VI	5.656	1.24	259	3.207	8.10
CUSPIDES	0.887	1.39	259	-1.851	3.62
AP	1.154	2.49	259	-3.743	6.05
summit	0.261	2.49	259	-4.636	5.16

Table 3. Bipolar amplitude for each isochrone with CL = 95%.

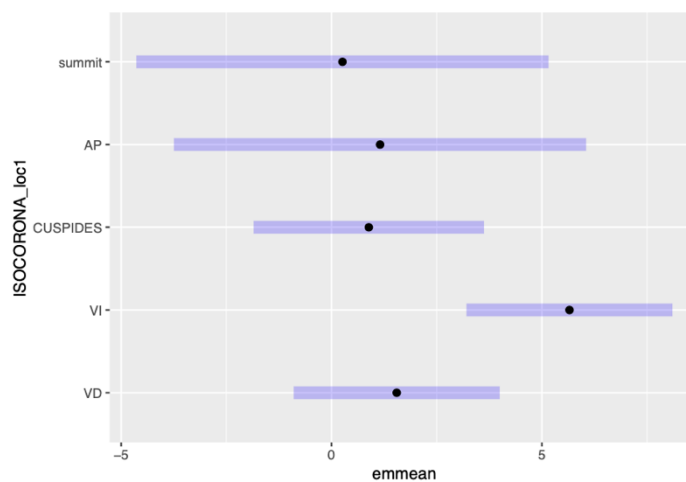


Figure 17. Amplitude of the bipolar signal.

5.3.2. Unipolar signal

For the study of the unipolar signals, we evaluated the number of unipolar negative deflections, the unipolar slope (amplitude of the negative drop vs negative precocity) and the absolute unipolar precocity respect the QRS activation, for the comparison of the right and left ventricles.

First of all, we assessed the number of unipolar negative deflections. We found that the areas presenting the largest average of unipolar negative deflections were the right ventricle (VD, 1.43 +/- 0.0765), the cusps (CUSPIDES, 1.53 +/- 0.0856) and the pulmonary arteries (AP, 1.65 +/- 0,1531). (Table 4 and figure 18)

ISOCORONA_loc1	emmean	SE	df	lower.CL	upper.CL
VD	1.43	0.0765	259	1.277	1.58
VI	1.24	0.0765	259	1.087	1.39
CUSPIDES	1.53	0.0856	259	1.363	1.70
AP	1.65	0.1531	259	1.349	1.95
summit	0.95	0.1531	259	0.649	1.25

Table 4. Number of unipolar negative deflections for each of the most precocious isochrones.

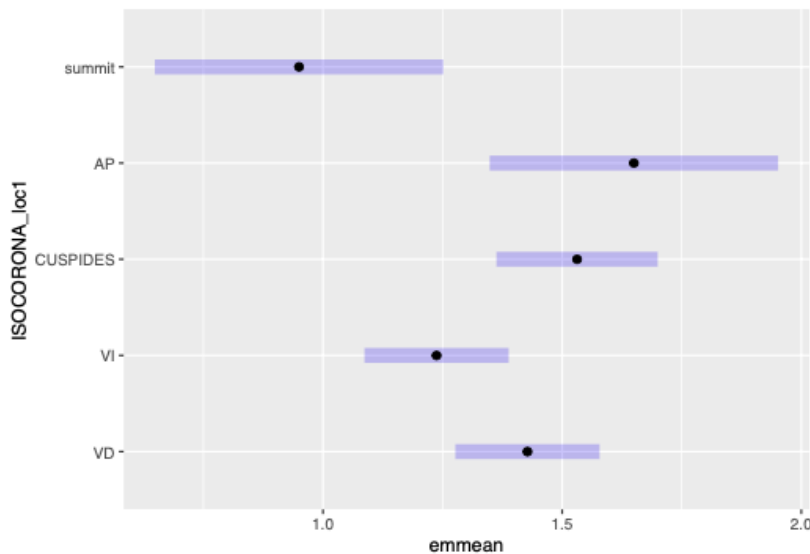


Figure 18. Plot representing the expected amount of unipolar negative deflections per isochrone.

The increase of the number of unipolar negative deflections has been found to be statistically significant between these three areas and the summit (whose average of negative deflections was 0.95 +/- 0.1531), VD vs. summit (p = 0.0445), cusps vs. summit (p = 0.0092) and AP vs. summit (p = 0.0119).

contrast	estimate	SE	df	t.ratio	p.value
VD - VI	0.190	0.108	259	1.756	0.4020
VD - CUSPIDES	-0.104	0.115	259	-0.904	0.8953
VD - AP	-0.222	0.171	259	-1.300	0.6913
VD - summit	0.477	0.171	259	2.790	0.0445
VI - CUSPIDES	-0.294	0.115	259	-2.559	0.0812
VI - AP	-0.412	0.171	259	-2.411	0.1157
VI - summit	0.287	0.171	259	1.680	0.4481
CUSPIDES - AP	-0.119	0.175	259	-0.677	0.9612
CUSPIDES - summit	0.581	0.175	259	3.315	0.0092
AP - summit	0.700	0.216	259	3.234	0.0119

Table 5. Contrast of the unipolar negative deflections by isochrone.

We, then, measured the slope of the unipolar signal, which was obtained through the relation between the amplitude of the unipolar negative deflection (from its positive to its negative peaks) and the elapsed period between the first unipolar activation and the minimum unipolar potential measured.

The results obtained showed that the steepest slope appeared in the left ventricular area (0.3085mV/ms), whereas the flattest slope was found in the summit (around 0.03mV/ms). The slopes measured for the other cardiac structures ranged between 0.083mV/ms and 0.15mV/ms.

ISOCORONA_loc1	emmean	SE	df	lower.CL	upper.CL
VD	0.0925	0.0551	255	-0.0161	0.201
VI	0.3085	0.0558	255	0.1986	0.418
CUSPIDES	0.0832	0.0621	255	-0.0392	0.206
AP	0.1506	0.1103	255	-0.0666	0.368
summit	0.0297	0.1131	255	-0.1931	0.252

Table 6. Unipolar signal slopes measured.

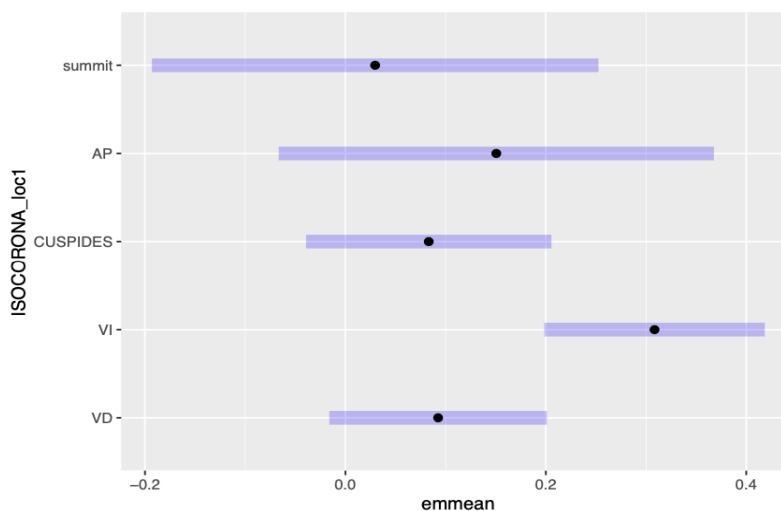


Figure 19. Plot showing the unipolar slopes measured with a 95% confidence interval.

We found that the differences observed between the slopes of the unipolar signals measured between the right and left ventricles were statistically significantly (0.0295 +- 0.0551 vs 0.3085 +- 0.0558, p = 0.0493). An other aspects to be noticed is that the differences in slope between the left ventricle and the cusps were almost significative (0.3085 +- 0.0558 vs 0.0832 +- 0.0621, p = 0.0571). (Table 6 and figure 19).

contrast	estimate	SE	df	t.ratio	p.value
VD - VI	-0.21599	0.0785	255	-2.753	0.0493
VD - CUSPIDES	0.00935	0.0831	255	0.113	1.0000
VD - AP	-0.05806	0.1233	255	-0.471	0.9899
VD - summit	0.06282	0.1259	255	0.499	0.9874
VI - CUSPIDES	0.22535	0.0835	255	2.698	0.0571
VI - AP	0.15793	0.1236	255	1.278	0.7051
VI - summit	0.27882	0.1262	255	2.210	0.1793
CUSPIDES - AP	-0.06742	0.1266	255	-0.533	0.9839
CUSPIDES - summit	0.05347	0.1291	255	0.414	0.9938
AP - summit	0.12088	0.1580	255	0.765	0.9403

Table 7. Contrast of the slopes of the unipolar signals between different cardiac structures.

Last, but not least, we compared differences in the unipolar precocities measured between the right and left ventricles to evaluate if the earliest activation differences between these areas were significative.

For the right ventricle we obtained a mean precocity of 26.9ms, whereas for the left ventricle earliest activations of 16.2ms were acquired.

The difference between both ventricles was statistically significant (p = 0.0002). (Table 8).

contrast	estimate	SE	df	t.ratio	p.value
VD - VI	10.621	2.44	259	4.357	0.0002

Table 8. Contrast between the unipolar signals from the right and left ventricles

We also tried to compare the results obtained with the characterization of PVCs and the long-term apparition of recurrences. Nevertheless, due to the lack of time to perform Holter monitoring at 3 and 6 months after the ablation, and the relatively small number of PVCs to analyse (29). The statistical analysis regarding these variables resulted in poor p-values and the inability to study the long-term apparition of recurrences and the study of the PVC characteristics for more concrete ventricular substructures other than LV, RV, PA, the summit and the cusps.

5.3.3. Other observations

As the evaluation of the long-term success of cardiac ablation is obtained by the use of 3-month and 6-month Holter examination on the patient, the evaluation of these data could not be done for all of the patients enrolled in this project, resulting in an incomplete evaluation of the long-term role of the multiple unipolar deflection on the success of RF ablation.

5.4. Discussion

On the whole of this project, we have been able to study the ventricular electrophysiological interactions that take place during the generation of PVCs. Firstly, we classified the isochrones where PVCs were generated in 5 main structures (VD, VI, AP, summit and cusps). Our relatively small number of samples ($n = 29$) was enough to evaluate if the morphology of the intracavitary signals, that appeared during the ablation procedure, was different enough between these structures to suggest that the structure where the PVC is generated influences its characteristics. Potentially, it could be used as a marker of the outcome of the ablation, but further studies are needed. However, the 5 main locations that we studied could be divided in almost 20 different substructures. Meaning that further studies, evaluating the intracavitary signal modification on specific ventricular location of the isochrones, need a fairly larger number of samples.

Ventricles

Regarding the results obtained from the study of bipolar signal, we observed that the smallest measurement of the earliest activation was found at the left ventricle (24.4ms). The structures found at the left ventricles, such as the papillary muscles, or the thickness of its walls could be obstacles to the transmission of low amplitude precocities, resulting in later activations than the other causing the PVC.

On the other hand, the left ventricle (LV) presented the largest bipolar amplitude (3.65 times bigger than the second one, the right ventricle (RV)). Meaning that bipolar amplitudes measured there should be expected to be much larger than the ones measured in the other structures.

The combination of the largest amplitude and the smallest precocity resulted in the steepest slope measured.

Other results of interest were the significance of the comparison between the precocities of the and LV the summit. This result could be used to assess that if large bipolar activation differences, about 18-20ms, are observed between these 2 areas, we could consider the PVC ablation of this area to be in advanced stages (or even finished).

For the right ventricle, the mean number of unipolar negative deflections was 1.43. Values closer to a 1.5 mean suggest that there were observed the same number of isolated negative deflections and multiple negative deflections, so the detection of this morphology on the right ventricles on an ablated tissue could be considered as normal.

The comparison of the results for these 2 structures was interesting, as we observed that the comparison of the bipolar precocities between the ventricles were estimated at 8.588ms, which was an almost significative contrast. We decided to also compare their unipolar precocities to confirm if their differences in temporal activation could give out information about the intervention. We found significant differences in unipolar precocities. Bipolar and unipolar activations spaced around 9 and 4ms, respectively, between the ventricles could be used as a marker of the state of completion of the intervention. The slope of the signals

detected at the ventricles could also be an interesting biomarker, as notably larger slopes should be expected at the LV when compared to the RV.

A reason that could explain these important interventricular variations is that the right and left ventricles are not formed by the same kind of tissues, with the left ventricle having a wall that can be as three times thicker than the right ventricular one, so there are ground that could lead to expect different measurements for different ventricles.

Nevertheless, further studies are needed to either confirm or reject the magnitude of the ventricular precocities for being used as a marker of the state of the ablation.

Pulmonary Artery (PA) and cusps

We observed that the main ventricular main ventricular blood vessels showed a similar behaviour that differed from the rest of the ventricular structures. Their comparison showed no differences ($p\text{-value} > 0.95$) in mainly all the variables tested, meaning that both tissues have an almost identical response to PVC and PVC ablation.

The PA and the cusps are both formed by non-conductive tissue that difficult the transmission of electrical stimuli which resulted in bipolar precocities between 25 and 30ms. Interestingly, these activations are similar to the ones measured for the LV, which made us think that further studies could assess the response of non-conductive tissue and the thick conductive tissue of the LV to low amplitude ventricular precocities.

The mean number of negative unipolar deflections for these 2 areas was higher than 1.5. These measures resulted in a significant difference when compared to the summit (whose mean number of negative deflections is almost 1) so the increase of negative deflections was not caused by chance. The noticing of more multiple unipolar negative deflections than single negative deflection signals might be used as a marker of the finalization of the ablation procedure

Summit

Finally, the summit showed notably different results than the rest of the structures. We found that this area presented the smallest amplitudes recorded, with a mean of 0.3mV but the largest bipolar precocities. Resulting in an area where stimuli appear the furthest from the PVC but present really low potential.

The average number of negative deflections of the signals found in this area was close to 1, so the signals be found at this area will be expected to show only one negative tension peak and flatter slopes than the rest of the areas, with an average slope of almost 0mV/ms (0.03mV/ms).

5.5. Limitations of our study

The main limitations that we faced and that did not let us achieve the full scope of the project were:

1. The number of patients and PVC list large enough to study the electrophysiological characteristics of the 5 main areas in which we divided the ventricles. However, it was not large enough to characterize the ventricular substructures.
2. The amount of time that we had. We did not have enough time to perform 3-month and 6-month Holter, we cannot correlate the success of the ablation with the studied biomarkers.

6. Execution chronogram

6.1. Work breakdown structure (WBS)

A WBS is a structure used for organizing and distributing the different stages through which we will during the development of the project and their subphases aiming for its success.

It consists of 2 main parts: first of all, figure x shows a schematic description of the different stages and breakpoints in which we have decided to segment our project. Then, we can find the WBS dictionary, which is a more detailed description of the breakpoints aforementioned as well as an identification that will be used to identify each task when we talk about them in the GANTT and PERT charts.

We have decided to divide the tasks of the project in 5 main phases that will be used to separate different processes.

In the first phase we wanted to define all the fundamentals of the project and assess its environment. Then, we proceeded to collect the number of available PVC cases since 2019 and begun its study using CARTO. The third and main experimental phase of the project was targeted the acquisition and study of the whole of the data of the project.

After finishing the experimental part, the next phase comprised tasks that regarded the analysis of the data and the obtention of the results for the completion of the project.

Finally, the last phase consisted on the presentation of the document and its exposition.

WBS of the study



Figure 20. WBS of the project indicating the main phases and tasks.

6.1.2. Coding the tasks

In the following table we have all the tasks indexed. They have been assigned a letter that will be used for their recognition in future tasks.

Reference WBS	Code	Activity
Phase 1	-	-
1.1	A	Goals
1.2	B	State of the art
1.3	C	Market Analysis
Phase 2		
2.1	D	List of cases
2.2	E	Conception Engineering
2.3	F	CARTO learning curve
Phase 3	-	-
3.1	G	Map merging
3.2	H	Study of the maps
3.3	I	Detail Engineering
Phase 4	-	-
4.1	J	Data analysis
4.2	K	Results and discussion
4.3	L	End of the report
Phase 5	-	-
5.1	M	Send the report
5.2	N	Presentation
5.3	O	Closure

Table 9. Tasks classified by which phase they belong and coded for its easier recognition.

6.1.3. Definition of the times:

This section will show the time needed for the completion of each task. The time expected for the completion of each task will be estimated following the mean calculation of 3 parameters: the **Pessimistic time (PT)**, which is the maximum time in which the task is expected to be completed, the **Optimistic time (OT)**, which is the least amount of time in which the task is expected to be completed and the **Probable time (PrT)** which is an amount of time between the pessimistic and the optimistic one in which the task will probably be completed.

The mean calculation of these 3 times will give us the **Expected time value (ET)**. The amount of time calculated to be needed for each task is shown in table 2.

All the amounts of time are defined in hours.

Activity code	OT (h)	PrT (h)	Pt (h)	Et (h)
A	2.5	4	6	4.17
B	9	12	18	13
C	7	11	14	10.67
Phase 1	18.5	27	38	27.83
D	1	3	5	3
E	7	10	14	10.33
F	14	19	25	19.33
Phase 2	22	32	44	32.67
G	7	10	15	10.67
H	30	45	55	43.33
I	12	20	30	20.67
Phase 3	49	75	100	74.67
J	5	10	12	9
K	6	10	14	10
L	5	10	20	11.67
Phase 4	16	30	46	30.67
M	0.5	1	3	1.5
N	2	5	8	5
O		-		
Total	108	170	239	172.33

Table 10. Estimation of the time needed for the completion of the project

From the table we can see that the expected time for the completion of the different tasks of the project will be between 27 and 28 hours for the first planification phase (Phase 1), between 32 and 33 working hours for the second conception and learning phase (Phase 2). These 2 phases will be followed by the bulk of the project, which will be the detailed study of all the 29 cases that we will be studying (Phase 3). This stage will have a length of approximately 75 working hours. The second to last phase (Phase 4) will be the completion of the analyses the report, which is expected to last around 31 working hours. Finally, we find the presentation of the project, which is expected to last 6.5 working hours.

Taking into account all the time frames in which we can find ourselves into, the total amount of hours which this project is expected to last is around 172 working hours.

6.2. Dependency matrix

This section consists of the linking of the different breakpoints of our project so that we can assess which tasks depend on the completion of previous breakpoints before they begin, and which them can be done parallelly. That way we will be able to assess the minimum and maximum times needed for the completion of the project. These aspects will be graphically shown in the following PERT and GANTT diagrams.

Code	Activity	Precedence
A	Goals	-
B	State of the art	A
C	Market Analysis	A
D	List of cases	B, C
E	Conception Engineering	D
F	CARTO learning curve	E
G	Map merging	F
H	Study of the maps	G
I	Detail Engineering	H
J	Data analysis	I
K	Results and discussion	J
L	End of the report	K
M	Send the report	L
N	Presentation	L
O	Closure	M, N

Table 11. Definition of the precedencies of each task.

6.3. PERT diagram

The PERT chart is a tool used for estimating the length of each of the phases of a project, analyzing the timeline of a project and the dependencies, we can assess which tasks of our project can be done at the same time and which ones depend on other tasks before they can even begin.

By using PERT charts, we can evaluate the sequential timeline of the tasks and when they must be completed for the project to go on. That is known as the critical path, which is the minimum amount of time that our project needs in order to be completed.

As it can be seen in our diagram, the critical paths for the completion of the project will need of a minimum of 148 working hours. For the estimation of these parameters, we used the values of the expected times.

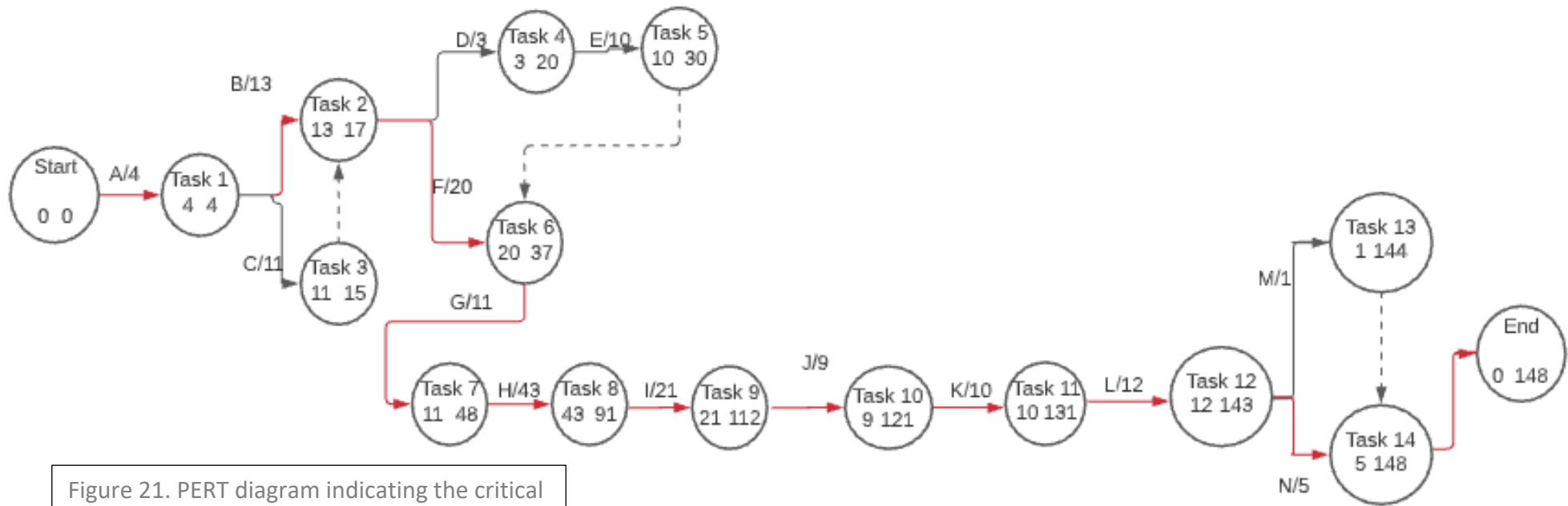


Figure 21. PERT diagram indicating the critical path.

6.4. GANTT diagram

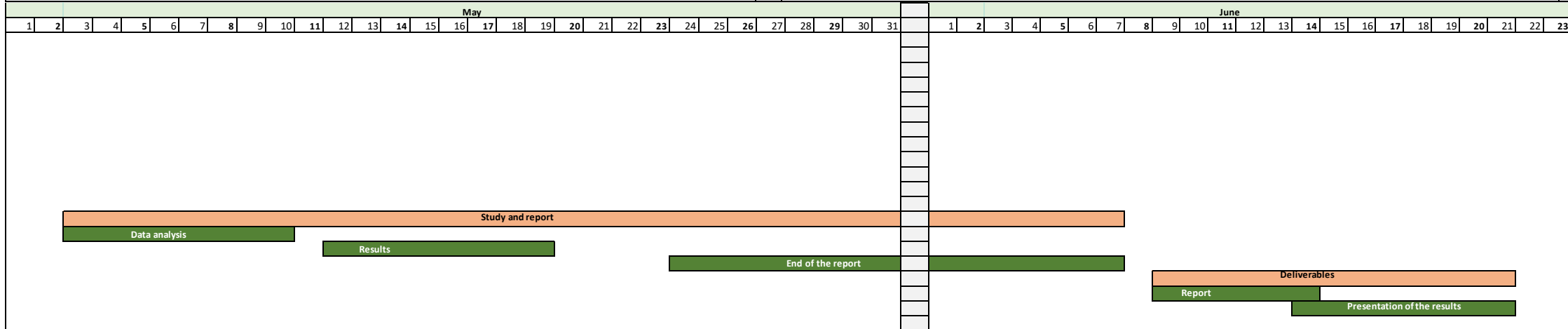
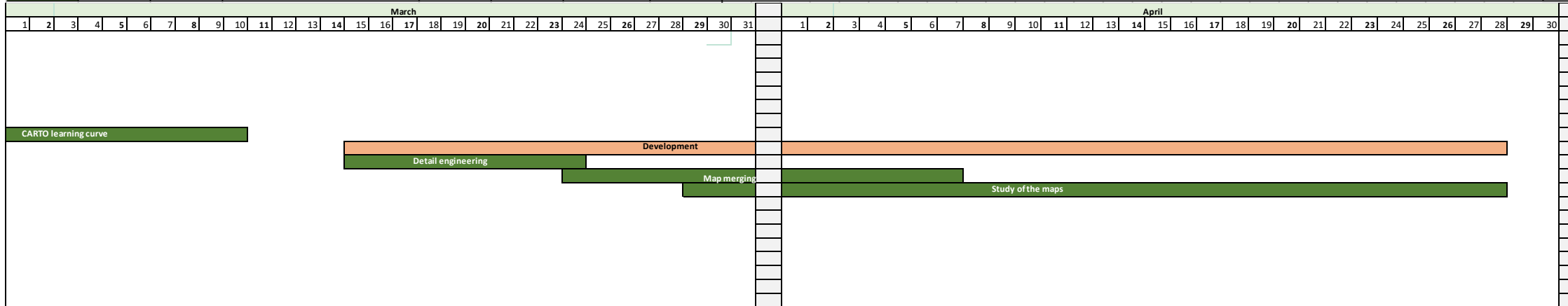
In our final planification of the times needed for the execution of the project we have done a GANTT chart, which consists of another way to represent the completion of each activity of our project against time.

From left to right it is composed of the activities that will be done, the date on which those activities are expected to start and a bar that represents the amount of time that those tasks are expected to occupy. At the beginning of the GANTT diagram, we have specified the date in which the project began, which was on February 2nd, 2021.

From the following chart, we can also see the length of each of the phases, with the lengthiest of them being the Development phase, needing around a month and a half to be finished.

The whole project ended on June 21st, 2021. Having a span of 4 months and 20 days.

Colour	WBS number	Task	Date of start	Planned end d	Duration (hours)	GANTT CHART	February																															
							1	2	3	4	5	6	7	8	9	10	11	12	13	14	15	16	17	18	19	20	21	22	23	24	25	26	27	28				
	1	Beginning	1/2/21	17/2/21	28		Beginning																															
	1.1	Goals	1/2/21	8/2/21	4		Goals																															
	1.2	State of the art	8/2/21	17/2/21	13																																	
	1.3	Market analysis	8/2/21	15/2/21	11																																	
	2	Approach to the study	18/2/21	10/3/21	33																																	
	2.1	List of cases	18/2/21	18/2/21	3																																	
	2.2	Conception engineering	18/2/21	24/2/21	10																																	
	2.3	CARTO learning curve	24/2/21	10/3/21	20																																	
	3	Development	15/3/21	28/4/21	75																																	
	3.1	Detail engineering	15/3/21	24/3/21	11																																	
	3.2	Map merging	24/3/21	7/4/21	43																																	
	3.3	Study of the maps	29/3/21	28/4/21	21																																	
	4	Study and report	3/5/21	7/6/21	31																																	
	4.1	Data analysis	3/5/21	10/5/21	9																																	
	4.2	Results	12/5/21	19/5/21	10																																	
	4.3	End of the report	24/5/21	7/6/21	12																																	
	5	Deliverables	9/6/21	21/6/21	20																																	
	5.1	Report	9/6/21	14/6/21	1.5																																	
	5.2	Presentation of the results	14/6/21	21/6/21	5																																	
	5.3	Closure	21/6/21	21/6/21	0																																	



7. Technical viability

This section is dedicated to analyse the different variables, internal or external, that can affect the development of the project.

To do so, we have classified the factors in the environment in a SWOT analysis, that organizes these variables depending on if they suppose a Strength, a Weakness, an Opportunity or a Threat for the project.

1. **Strengths:** The main strengths of our project are the situation in which it has been performed, this being the Arrhythmia Unit of the Hospital Clínic of Barcelona, which possesses very experimented professionals that work with electrophysiological cardiac conditions daily, an often with the treatment of PVCs. This unit also has facilities necessary for performing the intervention and the material, this being ablation and magnetic catheters, mapping software, pacing devices, et cetera.
2. **Weaknesses:** The principal weaknesses that the project faces are that some of the studied maps might not have enough point for them to be studied in depth or that the unipolar signals measured are not stable enough to ensure a satisfactory study of the points; for example, the signals can be saturated, noisy or even both, troubling the characterization of some of the morphological measurements of the unipolar signal.
3. **Opportunities:** The biggest opportunities in our scope are the small number of studies that have been made regarding the influence of unipolar signal morphology in the result of cardiac catheter ablation and that none of them, at least that we know of, has been made studying the double drop of the unipolar signal.
4. **Threats:** The data obtained relies greatly on the criteria of the operator, so the data obtained can differ depending on the operator.

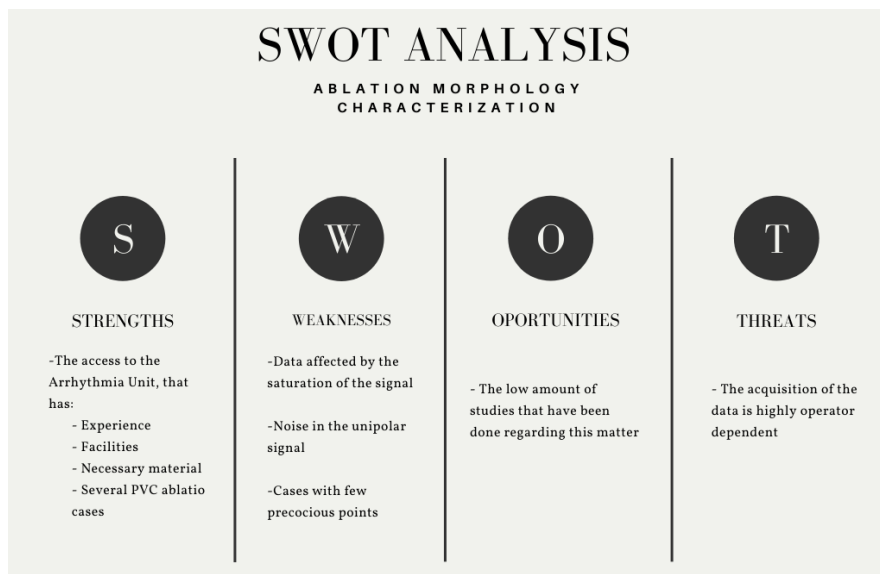


Figure 22. SWOT analysis of the environment of our project

8. Economic viability

As the unit where this project has taken place already had all the materials and software needed for the ablations and all the interventions studied had already been done prior to the start of the study, no new material had to be bought and no new interventions were made. All of these aspects resulted no added cost for the realization of the study.

9. Laws to which the study is subjected

The full procedure included in this project has been done under the General Data Protection Regulation (GDPR) of the European Union. This law came into force for all the integrating states of the EU on May 25th 2018^[58].

The setting in which this law affects medical studies is that the clinical data that is being used cannot be tracked up to the patient from which it was obtained. For our study, ablation data has been dissociated from the patient.

Patients that have been part of our project freely signed an informed consent stating the use that could be done with the data obtained from the ablation of their PVCs.

10. Conclusions and future lines

All in all, our study attempted to characterize the signals belonging to the earliest activations of the cardiac tissue that produced PVCs.

We found hints suggesting that the characteristics of the intracavitary signals collected during an ablation procedure could be used to evaluate the stage of the intervention, and that for different cardiac tissues several unipolar and bipolar signal morphologies are expected to be found, finding significant results for the main 5 areas that can cause PVCs.

Our main limitations were the lack of time to perform 3 and 6-month post-ablation Holters on patients, aiming to evaluate our results against long-term apparition of recurrences. A larger sample of PVCs would also be needed to evaluate different signal morphologies from the cardiac substructures.

Future studies regarding unipolar and bipolar ablation signals could focus on the study of the long-term outcomes of the ablation procedure such as the PVC burden and the apparition of recurrences or the characterization of ventricular substructures.

To conclude, the results of our study suggest that the morphological characteristics of the ablation procedure could be used as markers for future interventions. Nevertheless, further studies need to be done to check which concrete role these signals have in the assessment of PVC ablation.

11. Bibliography

1. Tan CMJ, Lewandowski AJ. The Transitional Heart: From Early Embryonic and Fetal Development to Neonatal Life. *Fetal Diagn Ther.* 2020;47(5):373-386..
2. Desai DS, Hajouli S. Arrhythmias. 2020 Dec 25. In: StatPearls [Internet]. Treasure Island (FL): StatPearls Publishing; 2021 Jan–. PMID: 32644349.
3. Cronin EM, Bogun FM, Maury P, Peichl P, Chen M, Namboodiri N, Aguinaga L, Leite LR, et al; ESC Scientific Document Group. 2019 HRS/EHRA/APHRS/LAHS expert consensus statement on catheter ablation of ventricular arrhythmias. *Europace.* 2019 Aug 1;21(8):1143-1144. doi: 10.1093/europace/euz132. Erratum in: *Europace.* 2019 Aug 1;21(8):1144. Erratum in: *J Arrhythm.* 2020 Jan 12;36(1):214. Erratum in: *Europace.* 2020 Mar 1;22(3):505. PMID: 31075787; PMCID: PMC7967791.
4. O'Quinn MP, Mazzella AJ, Kumar P. Approach to Management of Premature Ventricular Contractions. *Curr Treat Options Cardiovasc Med.* 2019 Sep 5;21(10):53.
5. Al-Khatib SM, Stevenson WG, Ackerman MJ, Bryant WJ, Callans DJ, Curtis AB, et al, Page RL. 2017 AHA/ACC/HRS guideline for management of patients with ventricular arrhythmias and the prevention of sudden cardiac death: Executive summary: A Report of the American College of Cardiology/American Heart Association Task Force on Clinical Practice Guidelines and the Heart Rhythm Society. *Heart Rhythm.* 2018 Oct;15(10):e190-e252. doi: 10.1016/j.hrthm.2017.10.035. Epub 2017 Oct 30. Erratum in: *Heart Rhythm.* 2018 Sep 26;: PMID: 29097320.
6. Latchamsetty R, Bogun F. Premature Ventricular Complex-Induced Cardiomyopathy. *JACC Clin Electrophysiol.* 2019 May;5(5):537-550.
7. Guandalini GS, Liang JJ, Marchlinski FE. Ventricular Tachycardia Ablation: Past, Present, and Future Perspectives. *JACC Clin Electrophysiol.* 2019 Dec;5(12):1363-1383.
8. Tung R, Boyle NG, Shivkumar K. Catheter ablation of ventricular tachycardia. *Circulation.* 2011 May 24;123(20):2284-8.
9. Stevenson WG, Friedman PL, Sager PT, Saxon LA, Kocovic D, Harada T, et al. Exploring postinfarction reentrant ventricular tachycardia with entrainment mapping. *J Am Coll Cardiol.* 1997 May;29(6):1180-9.
10. Callans DJ, Zado E, Sarter BH, Schwartzman D, Gottlieb CD, Marchlinski FE. Efficacy of radiofrequency catheter ablation for ventricular tachycardia in healed myocardial infarction. *Am J Cardiol.* 1998 Aug 15;82(4):429-32.

11. M.V. Cañadas Godoy, A.C. Martín García, H.D. Mejía Rentería, N. Pérez Castellano, J. Pérez-Villacastín. Taquiarritmias y muerte súbita. En: M.A. García Fernández, L. Pérez de Isla, J.J. Gómez de Diego. Coordinators. Tratado de Cardiología Clínica, volumen I y II. Grupo CTO editorial. P: 341 – 354.
12. Zhao Z, Liu X, Gao L, Xi Y, Chen Q, Chang D, et al. Benefit of Contact Force-Guided Catheter Ablation for Treating Premature Ventricular Contractions. *Tex Heart Inst J.* 2020 Feb 1;47(1):3-9.
13. Mullis AH, Ayoub K, Shah J, Butt M, Suffredini J, Czarapata M, Delisle B, Ogunbayo GO, Darrat Y, Elayi CS. Fluctuations in premature ventricular contraction burden can affect medical assessment and management. *Heart Rhythm.* 2019 Oct;16(10):1570-1574.
14. A Perez-Silva. Jose Luis Merino. Frequent ventricular extrasystoles: significance, prognosis and treatment. *Journal of the ESC Council for Cardiology Practice.* Jan 2011. Vol. 9, N° 17 - 28. Available in: <https://www.escardio.org/Journals/E-Journal-of-Cardiology-Practice/Volume-9/Frequent-ventricular-extrasystoles-significance-prognosis-and-treatment>
15. Farzam K, Richards JR. Premature Ventricular Contraction. 2021 Feb 2. In: *StatPearls [Internet]. Treasure Island (FL): StatPearls Publishing; 2021 Jan–.* PMID: 30422584.
16. Author: Antonis S Manolis, Section Editor: Hugh Calkins, Deputy Editor: Todd F Dardas. Premature ventricular complexes: Treatment and prognosis. Wolters Kluwer. Jan. 2021
17. C. Ferrera Durán, A. Saltijerán Cerezo, M.A. García Fernández, C. Macaya Miguel. Farmacología clínica cardiovascular. En: M.A. García Fernández, L. Pérez de Isla, J.J. Gómez de Diego. Coordinators. Tratado de Cardiología Clínica, volumen I y II. Grupo CTO editorial. P: 105 – 132.
18. A. Estrada Mucci, J. Figueroa, S. Castrejón-Castrejón, J.L. Merino Llorens. Estudio electrofisiológico y ablación. Cardioversión eléctrica y test farmacológicos en arritmias. En: M.A. García Fernández, L. Pérez de Isla, J.J. Gómez de Diego. Coordinators. Tratado de Cardiología Clínica, volumen I y II. Grupo CTO editorial. P: 355 – 376.
19. Venkatachalam KL, Herbrandson JE, Asirvatham SJ. Signals and signal processing for the electrophysiologist: part II: signal processing and artifact. *Circ Arrhythm Electrophysiol.* 2011 Dec;4(6):974-81.

20. Meloni MF, Chiang J, Laeseke PF, Dietrich CF, Sannino A, Solbiati M, et al. Microwave ablation in primary and secondary liver tumours: technical and clinical approaches. *Int J Hyperthermia*. 2017 Feb;33(1):15-24.
21. Kay GN, Epstein AE, Bubien RS, Anderson PG, Dailey SM, Plumb VJ. Intracoronary ethanol ablation for the treatment of recurrent sustained ventricular tachycardia. *J Am Coll Cardiol*. 1992 Jan;19(1):159-68.
22. Cuculich PS, Schill MR, Kashani R, Mutic S, Lang A, Cooper D, et al. Noninvasive Cardiac Radiation for Ablation of Ventricular Tachycardia. *N Engl J Med*. 2017 Dec 14;377(24):2325-2336.
23. Sharma A, Wong D, Weidlich G, Fogarty T, Jack A, Sumanaweera T, Maguire P. Noninvasive stereotactic radiosurgery (CyberHeart) for creation of ablation lesions in the atrium. *Heart Rhythm*. 2010 Jun;7(6):802-10.
24. Soucek F, Starek Z. Use of Bipolar Radiofrequency Catheter Ablation in the Treatment of Cardiac Arrhythmias. *Curr Cardiol Rev*. 2018;14(3):185-191.
25. <https://www.heartrhythmclinic.com.au/arrhythmias/vt-in-structural-heart-disease/>, consulted on December 10th 2020.
26. Lee D, Hoffmayer KS, Hsu JC, Schricker A, Birgersdotter-Green U, Raissi F, et al. Long-term mode and timing of premature ventricular complex recurrence following successful catheter ablation. *J Interv Card Electrophysiol*. 2019 Aug;55(2):153-160.
27. Han D, Bashar SK, Mohagheghian F, Ding E, Whitcomb C, McManus DD, et al. Premature Atrial and Ventricular Contraction Detection using Photoplethysmographic Data from a Smartwatch. *Sensors (Basel)*. 2020 Oct 5;20(19):5683.
28. Corrado D, Drezner JA, D'Ascenzi F, et al. How to evaluate premature ventricular beats in the athlete: critical review and proposal of a diagnostic algorithm *British Journal of Sports Medicine* 2020; **54**: 1142-1148.
29. Loh P, van Es R, Groen MHA, Neven K, Kassenberg W, Wittkamp FHM, et al. Pulmonary Vein Isolation With Single Pulse Irreversible Electroporation: A First in Human Study in 10 Patients With Atrial Fibrillation. *Circ Arrhythm Electrophysiol*. 2020 Oct;13(10):e008192.

30. Kanat S, Duran Karaduman B, Tütüncü A, Tenekecioğlu E, Mutluer FO, Akar Bayram N. Effect of Echocardiographic Epicardial Adipose Tissue Thickness on Success Rates of Premature Ventricular Contraction Ablation. *Balkan Med J.* 2019 Oct 28;36(6):324-330.
31. Gargiulo GD. True unipolar ECG machine for Wilson Central Terminal measurements. *Biomed Res Int.* 2015;2015:586397.
32. <https://thoracickey.com/principles-and-techniques-of-cardiac-catheter-mapping/>. Consulted on April 2nd, 2021
33. Bazan V, Frankel DS, Santangeli P, Garcia FC, Tschabrunn CM, Marchlinski FE. Three-dimensional myocardial scar characterization from the endocardium: Usefulness of endocardial unipolar electroanatomic mapping. *J Cardiovasc Electrophysiol.* 2019 Mar;30(3):427-437.
34. <http://www.medicine.mcgill.ca/physio/vlab/cardio/ecgbasics.html>. Consulted on May 31st, 2021
35. Maury P, Monteil B, Marty L, Duparc A, Mondoly P, Rollin A. Three-dimensional mapping in the electrophysiological laboratory. *Arch Cardiovasc Dis.* 2018 Jun-Jul;111(6-7):456-464.
36. Eitel C, Hindricks G, Dagues N, Sommer P, Piorkowski C. EnSite Velocity cardiac mapping system: a new platform for 3D mapping of cardiac arrhythmias. *Expert Rev Med Devices.* 2010 Mar;7(2):185-92.
37. Kumar S, Barbhaiya CR, Sobieszczyk P, Eisenhauer AC, Couper GS, Nagashima K, et al. Role of alternative interventional procedures when endo and epicardial catheter ablation attempts for ventricular arrhythmias fail. *Circ Arrhythm Electrophysiol.* 2015 Jun;8(3):606-15.
38. Kataria V, Berte B, Vandekerckhove Y, Tavernier R, Duytschaever M. Remote Magnetic versus Manual Navigation for Radiofrequency Ablation of Paroxysmal Atrial Fibrillation: Long-Term, Controlled Data in a Large Cohort. *Biomed Res Int.* 2017;2017:6323729.
39. Dos Reis JE, Soullié P, Battaglia A, Petitmangin G, Hoyland P, Josseaume L, et al. Electrocardiogram Acquisition During Remote Magnetic Catheter Navigation. *Ann Biomed Eng.* 2019 Apr;47(4):1141-1152.
40. Ben-Haim SA, Osadchy D, Schuster I, Gepstein L, Hayam G, Josephson ME. Nonfluoroscopic, in vivo navigation and mapping technology. *Nat Med.* 1996 Dec;2(12):1393-5.
41. Larsen TR, Saini A, Moore J, Huizar JF, Tan AY, Ellenbogen KA, Kaszala K. Fluoroscopy reduction during device implantation by using three-dimensional navigation. A single-center experience. *J Cardiovasc Electrophysiol.* 2019 Oct;30(10):2027-2033.

42. Nakagawa H, Ikeda A, Sharma T, Lazzara R, Jackman WM. Rapid high resolution electroanatomical mapping: evaluation of a new system in a canine atrial linear lesion model. *Circ Arrhythm Electrophysiol*. 2012 Apr;5(2):417-24.
43. Khaykin Y, Oosthuizen R, Zarnett L, Wulffhart ZA, Whaley B, Hill C, et al. CARTO-guided vs. NavX-guided pulmonary vein antrum isolation and pulmonary vein antrum isolation performed without 3-D mapping: effect of the 3-D mapping system on procedure duration and fluoroscopy time. *J Interv Card Electrophysiol*. 2011 Apr;30(3):233-40.
44. https://www.biosensewebster.com/documents/SmartTouch_brochure.pdf?Cache=3/9/2015 last consulted on may 29th 2021.
45. Page SP, Dhinoja M. SmartTouch™ - The Emerging Role of Contact Force Technology in Complex Catheter Ablation. *Arrhythm Electrophysiol Rev*. 2012 Sep;1(1):59-62.
46. Pinto Teixeira P, Silva Cunha P, Delgado AS, Pimenta R, Martins Oliveira M, Cruz Ferreira R. Cateter PentaRay na ablação de fibrilhação auricular persistente [PentaRay catheter in persistent atrial fibrillation ablation]. *Rev Port Cardiol*. 2016 Feb;35(2):121-3. Portuguese.
47. Huang LH, Gao MY, Zeng LJ, Xie BQ, Shi L, Wang YJ, et al. Role of the notched unipolar electrogram in guiding catheter ablation of frequent premature ventricular contractions originating from the ventricular outflow tract. *J Int Med Res*. 2020 Dec;48(12):300060520977634.
48. Ejima K, Higuchi S, Yazaki K, Kataoka S, Yagishita D, Kanai M, et al. Comparison of high-power and conventional-power radiofrequency energy deliveries in pulmonary vein isolation using unipolar signal modification as a local endpoint. *J Cardiovasc Electrophysiol*. 2020 Jul;31(7):1702-1708.
49. Ejima K, Kato K, Okada A, Wakisaka O, Kimura R, Ishizawa M, et al. Comparison Between Contact Force Monitoring and Unipolar Signal Modification as a Guide for Catheter Ablation of Atrial Fibrillation: Prospective Multi-Center Randomized Study. *Circ Arrhythm Electrophysiol*. 2019 Aug;12(8): e007311.
50. Ariyaratna N, Kumar S, Thomas SP, Stevenson WG, Michaud GF. Role of Contact Force Sensing in Catheter Ablation of Cardiac Arrhythmias: Evolution or History Repeating Itself? *JACC Clin Electrophysiol*. 2018 Jun;4(6):707-723.
51. de Bakker JM. Electrogram recording and analyzing techniques to optimize selection of target sites for ablation of cardiac arrhythmias. *Pacing Clin Electrophysiol*. 2019;42(12):1503-1516.

52. Shaurya K. Properties of the Cardiac Muscle | Cardiovascular System.
53. <https://www.teachpe.com/anatomy-physiology/the-heart-conduction-system>
Consulted on June 5, 2021.
54. <https://www.intechopen.com/books/adaptive-filtering-applications/adaptive-noise-removal-of-ecg-signal-based-on-ensemble-empirical-mode-decomposition> Consulted on June 5, 2021
55. E. H. Houssein, M. Kilany, A. E. Hassanien. ECG signals classification: a review. *International Journal of Medical Engineering and Informatics*. Jan. 2017
56. <https://litfl.com/ecg-limb-lead-reversal-ecg-library/> Consulted on June 5, 2021
57. https://hallaweb.jlab.org/experiment/g2p/survey/Yaw_Pitch_Roll_Rotations.pdf
Consulted on June 6, 2021.
58. <https://gdpr-info.eu/chapter-1/> Consulted on June 7th, 2021

12. ANNEXES

1. Cardiac conduction system

The heart is the main pump and muscle of the circulatory system and one of the main elements of the organism; that's why keeping it healthy and capable has always been one of the main objectives of medicine.

The pumping mechanism of the heart leads to the spreading of blood through all of the tissues present in our body.

This organ, at its resting state, is polarized at about -80mV. When it receives a set of electrical stimuli it is depolarized, producing the contraction of its different chambers (atria and ventricles) due to the conduction of the stimuli through the **cardiac conduction system**.

The heart's conduction system is mainly formed by two kinds of cells: firstly, **the pacemaker cells (specialized)**. These cells, mostly found in the sinoatrial node, possess automatism. This is an intrinsic mechanism that allows them to generate an action potential that, when it surpasses a certain voltage threshold, will be spread throughout the rest of the heart chambers.

As soon as the impulse gets transmitted, the **myocardial cells**, will be stimulated and the myocardial fibers contracted, causing the heartbeat.

Nevertheless, the generation of the impulse cannot spread through the whole muscle without some extra structures; these structures, such as the SA node, AV node and the bundle of His, form the **conduction system**. [11, 17, 18, 52]

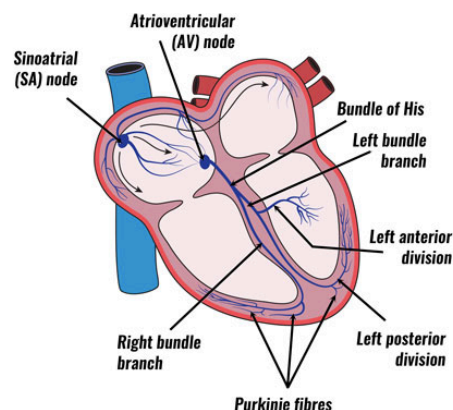


Figure 14. Cardiac conduction system. Image from^[53]

The **SA node** is where the pacemaker cells can be found and is the one that generates the usual electrical impulse of the heartbeat at a certain frequency, contracting the atria and causing the blood to reach the lower chambers of the heart. This impulse, then, travels onto the **AV node** and, from there, is transmitted through the bundle of His onto the Purkinje fibers that will depolarize and contract the ventricles. If this mechanism remains unaltered, the heart beats at a given frequency (beats per minute), called the **sinus rhythm**.

2. Arrhythmias

There are several mechanisms that may disrupt the pace of the conduction system and generate electrical impulses at different rates than the one set by the SA node.

These are dephased impulses that usually result in abnormal cardiac rhythms, called **arrhythmias**.^[2]

Depending on their frequency related to the sinus rhythm, arrhythmias can be classified into bradyarrhythmias (slower rhythm) and tachyarrhythmias (faster rhythm).

These processes form in many different ways, but they can be mainly divided in 3 groups:

- Reentries (they consist of abnormal circuits of propagation of the impulse caused that can take accessory paths of the myocardium and produce multiple stimulations of the tissue).
- Focal arrhythmias (a focus of the cardiac walls acquires automatism).
- Atrial fibrillation (extremely fast palpitations of the atria, usually coming from impulses generated on the pulmonary veins).

Arrhythmias can turn into cardiac conditions of considerable importance, so they have to be monitored and, in some cases, even treated.

3. Diagnosis of arrhythmias

The electrical nature of the heartbeat allows us to measure the impulse at each moment in time and assess its morphology which presents a set of wave patterns that when measured in an electrocardiogram (ECG) form a recognizable signal. These signals have mainly 5 different waves that appear as a result of the polarizations and depolarizations of the cardiac chambers (P, QRS, T). The P wave represents the depolarization of the atria. Then, we find the QRS complex, that represents the ventricular depolarization. These depolarizations are the source of the contraction of the chambers. Once the ventricles have contracted, the muscle relaxes, and the repolarization of the ventricles takes place, while waiting for the next depolarization. This phase is known as the refractory phase

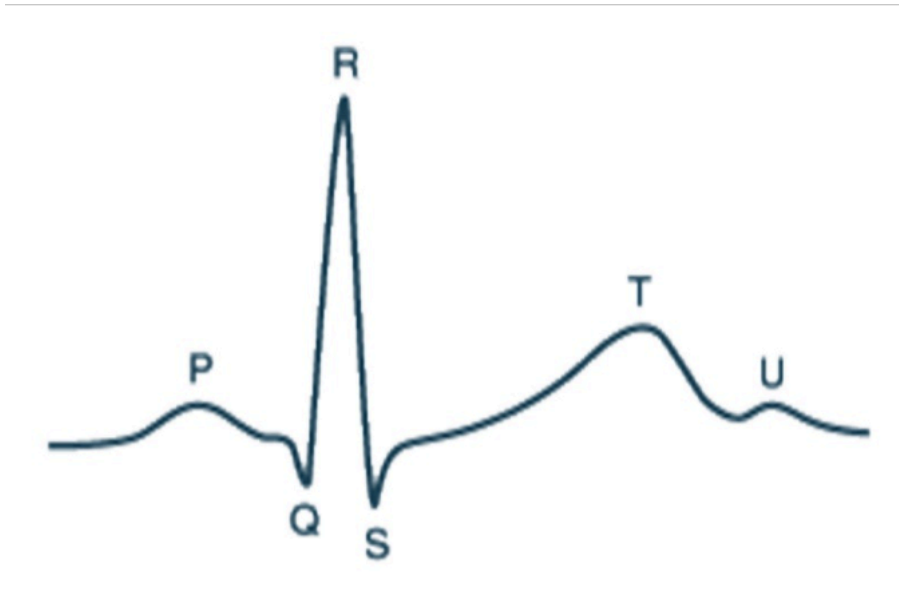


Figure 15. ECG sinus signal. Image from [54].

However, in arrhythmias, the measured signals differ from the usual QRS wave shape. Thus, the main procedure used for their diagnosis is the monitoring of the cardiac intrinsic signals and their morphology. The main diagnostic techniques are:

1. **Electrocardiogram (ECG):** An ECG consists of the measurement of the cardiac intrinsic depolarizations represented as waves. These are classified as **P-wave** (atrial depolarization), the **QRS complex** (ventricular depolarization) and the **T-wave** (ventricular repolarization). [55]

<i>Amplitude (mV)</i>	<i>Duration (seconds)</i>
P Wave – 0.25mV	PR interval – 0.12s to 0.20s
R Wave – 1.60mV	QT interval – 0.35s to 0.44s
Q Wave – 25% of R wave	ST interval – 0.05s to 0.15s
T Wave – 0.1 to 0.5mV	QRS interval – 0.09s

Table 4. Duration of the ECG-measured signals. Obtained from [55]

The obtention of this set of waves is achieved by the placement of 3 main differential electrodes on the right arm, RA, left arm, LA, and left leg, LL, of the patient forming what is known as the Einthoven triangle. Once the 3 differential electrodes are in place, the electrodes the potential measured between 2 of the 3 electrodes is compared to obtain the bipolar derivations, which are I (LA vs RA), II (RA vs LL) and III (LL vs LA). [56]

Then, unipolar derivations (aVL, aVR and aVF) can be obtained by comparing the potential measured at each single electrode vs the Wilson Central Terminal (which is obtained by combining the potential of all 3 electrodes (RA + LA + LL = 0)).

This leads us to 6 different derivations. For accomplishing a 12-lead ECG, 6 additional electrodes (V1-V6) are placed on the skin of the patient to obtain the 6 final derivations.

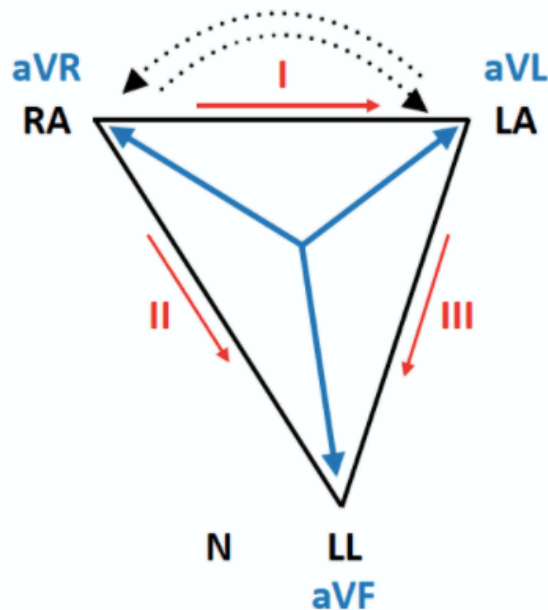


Figure 16. ECG unipolar and bipolar derivations. Image from [56]

2. **Holter:** Holters are devices used for arrhythmias that occur either sporadically or have a short duration. They consist of a small device and some electrodes that are placed on the skin of the patient; its main principle is a sustained obtention of an ECG, up to 24-48h, that can be useful for recording the ECG information at the time of the episode without the need for the patient to be at the hospital facilities.
3. **Implantable Holter:** Small device that uses 2 electrodes for ECG signal recording.

4. Pharmacological treatment of arrhythmias

When treating different medical conditions people tend to prefer treatments that do not imply the insertion of any device inside them. This results in the election of pharmacological antiarrhythmic treatment in the first instance in order to control the recurrence of the PVCs. There are 3 main kinds of medication used^[11, 17, 18]:

- Beta blockers: Their main effects rely on the suppression of the sympathetic nervous system at the beginning of arrhythmias caused by reentries as well as the ones caused by automatism. They reduce the activity of the SA and the AV nodes so that they can decrease the ventricular frequency.
- Sodium channel blockers: These medicines block the voltage-dependent Na-channels so that the myocardium can reduce its excitability, lowering the speed of the stimuli transmission
- Amiodarone: This drug is used for more resistant ventricular tachycardias. Its main effect is the increase of the refractory

period, thus, lowering the conduction time of the stimuli on the NAV

However, pharmacological treatments have a success rate between 15 - 65%, depending on the particularities of each case. Hence, for conditions that turn resistant to this treatment there is a more efficient treatment reserved as a second option due to its invasiveness.

5. RPY notation

Roll, Pitch and Yaw (RPY) notation is a terminology used to determine the three-dimensional rotation of a body across the three orthogonal axes (x,y,z).^[57]

Roll (R) is a 2D counterclockwise rotation of an angle γ respect to the X axis following a 2-dimensional rotation matrix as follows

$$R_x(\alpha) = \begin{pmatrix} \cos \alpha & -\sin \alpha & 0 \\ \sin \alpha & \cos \alpha & 0 \\ 0 & 0 & 1 \end{pmatrix}.$$

Expression 3. 2D rotation matrix across the x-axis, Roll.

Pitch is a counterclockwise rotation of an angle β respect to the Y axis.

$$R_y(\beta) = \begin{pmatrix} \cos \beta & 0 & \sin \beta \\ 0 & 1 & 0 \\ -\sin \beta & 0 & \cos \beta \end{pmatrix}.$$

Expression 4. 2D rotation matrix across the y-axis, Pitch.

Finally, Yaw represents a counterclockwise rotation of an angle α respect to the Z axis.

$$R_z(\gamma) = \begin{pmatrix} 1 & 0 & 0 \\ 0 & \cos \gamma & -\sin \gamma \\ 0 & \sin \gamma & \cos \gamma \end{pmatrix}.$$

Expression 5. 2D rotation matrix across the z-axis, Yaw.

These rotations *per se* do not define the three-dimensional rotation of a body, but the angles from each rotation can be combined to assess the final rotation of the body. Giving the RPY rotation as $R(\gamma)*P(\beta)*Y(\alpha)$.